NORSK POLARINSTITUTT

RAPPORTSERIE

NR. 98 - OSLO 1997

E. NØST & E. DYBESLAND

REVIEW OF SEA ICE DRIFT AND DISTRIBUTION IN THE FRAM STRAIT 1972-1994

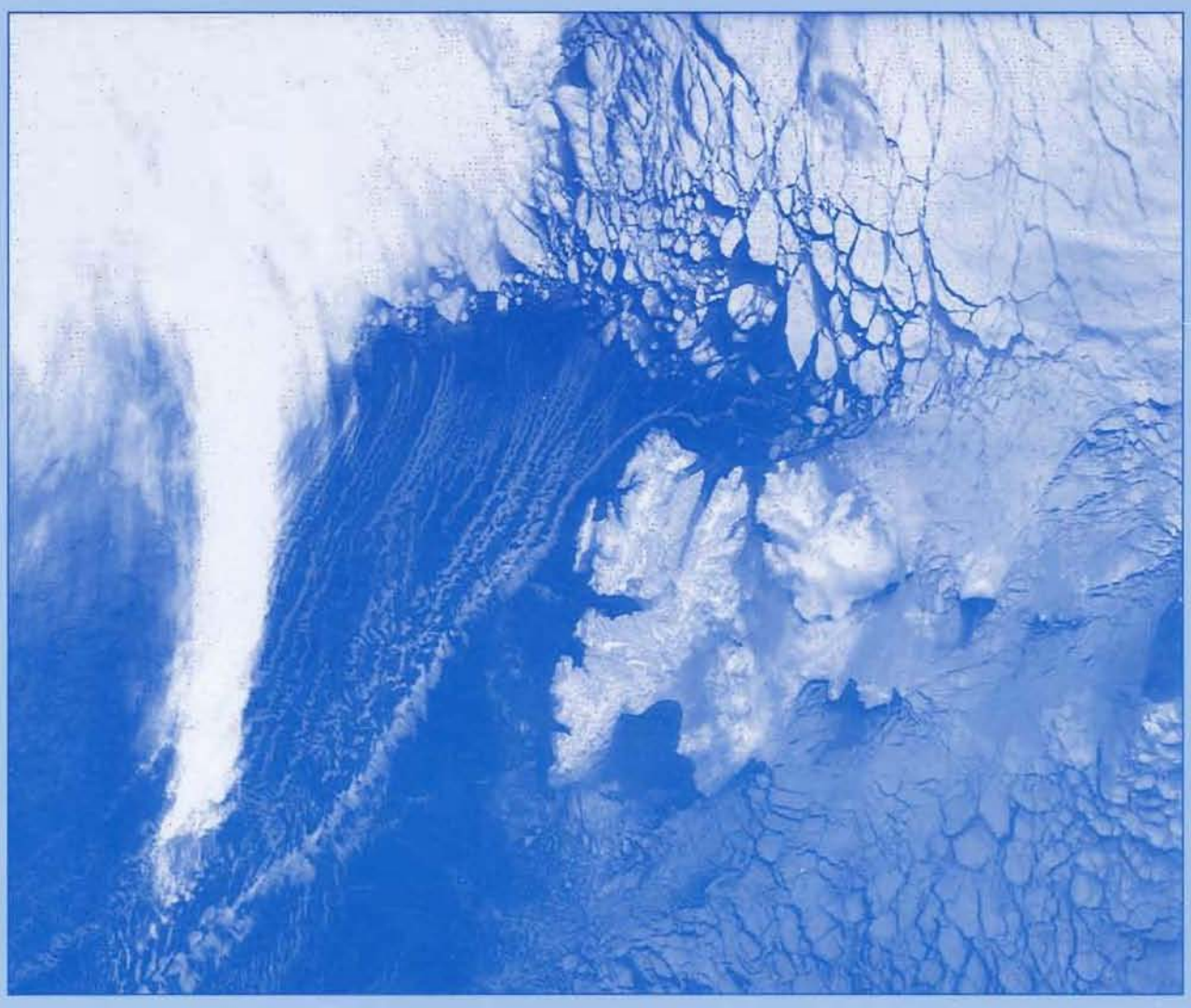

Rapport Nr. 98

E. NØST & E. DYBESLAND:

REVIEW OF SEA ICE DRIFT AND DISTRIBUTION IN THE FRAM STRAIT 1972-1994

NORSK POLARINSTITUTT
Oslo 1997

Elisabeth Nøst
SINTEF Applied Mathematics
P.O. Box 124, Blindern
N-0314 Oslo, Norway

Elen Dybesland
Det Norske Veritas Software
Veritasveien 1
1322 Høvik, Norway

© Norsk Polarinstitutt, Oslo
Printed July 1997
ISBN 82-7666-123-8

Cover: Temperature distribution in the Fram Strait and western Barents Sea as seen by NOAA satellite infrared sensor on 27 February 1987. Note the contrast between ice floes and the warmer water as well as the open water on the lee side of the islands. The imagery illustrates how ice from the Arctic Ocean is spreading out when passing through the Fram Strait, northwest of Svalbard (centre). Long cloud gates are formed where cold northerly winds pass over warmer water.

Abstract

Trajectories from drifting buoys on sea ice through Fram Strait for the years 1976-1994, from the International Arctic Buoy Program and Norsk Polarinstitutt, have been investigated focusing on ice drift, i.e ice velocity. Ice distribution, i.e. ice concentration data, from the Navy–NOAA Joint Ice Center Digitized Sea Ice Data is presented for the Fram Strait area for the years 1972–1990.

Histograms of drift velocities for all buoys, their seasonal and three-monthly mean values, the drifting buoys position and profiles showing number of buoys passing the specified latitudes are presented. Mean ice drift velocities is derived from the buoy velocities. Horizontal distribution of ice velocity, cross-strait profiles of ice velocity and ice concentration, and values of ice velocity, geostrophic wind and ice concentration at actual buoy positions are shown. Cross-strait variations of the meridional (south) component of the ice velocity which is computed in two different ways, are presented and compared to the ice velocities calculated by Vinje & Finnekåsa (1986).

Strong seasonal, inter annual and cross-strait variations in ice drift are found. During the winter season the sea ice motion is fast and straight forward in a wide ice stream. The ice drifts slower in a eddy structured and complex drift pattern during the summer season.

The NOAA Sea Ice Data contains weekly registrations of ice from January 1972 to April 1990. This work presents week-values of ice covered area and mean values averaged over months and year. The ice distribution in the Fram Strait is shown for special years were the distribution is deviated from the average. In general, the period with increasing area of ice cover in the Fram Strait starts in October and reaches a relatively stable maximum area in the period from December to March/April. The area covered with ice then decreases to a minimum in September.

This report also presents an overview of previous work done on sea ice in the Fram Strait and surrounding areas.

Contents

List of Figures

List of Tables

Chapter 1

Introduction

Sea ice is a thin, broken layer on the polar oceans which is modified in thickness and concentration by dynamic and thermodynamic processes. It represents the boundary between the atmosphere and ocean and influences their interaction considerably. Sea ice plays an important role in the climate system since it modifies the surface radiation balance due to its high albedo and since it effectively insulates the relative warm ocean from the atmosphere.

A given region may contain open water, young ice only a few centimeters thick, multi-year ice a few meters thick and pressure ice up to tens of meters thick (Thorndike et. al. 1975). Thermodynamic processes are responsible for mass changes at the upper and lower boundaries of the ice, and on a year long average strives for a single equilibrium thickness. Mechanical processes cause formation of leads and pressure ridges, and on a year long average, creates both thick pressure ice and open water (Thorndike et. al. 1975).

The sea ice cover is in continual motion driven by the atmosphere and ocean. Thorndike & Colony (1982) found that about a half of the average sea ice motion in the Arctic Ocean is directly related to the geostrophic wind, and the other half is due to the mean ocean circulation. Surface ocean currents account for about 80% of the ice motion when the sea ice passes through the Fram Strait (Vinje & Finnekåsa 1986). Ocean currents account for 30% of the ice motion at the Yermack Plateau during the period of time from September 20th to October 3rd 1991 (Sun & Askne 1995).

The mean annual large-scale drift of Arctic pack ice has two primary features (Figure 1.1) the Beaufort Gyre, an anticyclonic ice motion with a mean center at about 80°N, 155°W in the Canada Basin, and the Transpolar Drift Stream, a motion of ice away from the Siberian coast, across the North Pole and through the Fram Strait (Barry et. al. 1993; Colony & Thorndike 1984). Mean drift speeds are 1–3 cms^{-1} and 5–10 cms^{-1}, respectively, in the Beaufort Gyre and in the Transpolar Drift Stream (Barry et. al. 1993).

About 95% of the ice that leaves the Arctic Ocean passes through the Fram Strait (Vinje & Finnekåsa 1986), and Barry et. al. (1993) report that approximately 20% of the total ice covered area in the Arctic Basin annually exists through the Fram Strait, of which 80% consists of multi-year ice floes 2-3 meters thick (Gow & Tucker 1987). The Fram Strait is the key area for studying ice export from the Arctic, see Figure 1.1 (from International

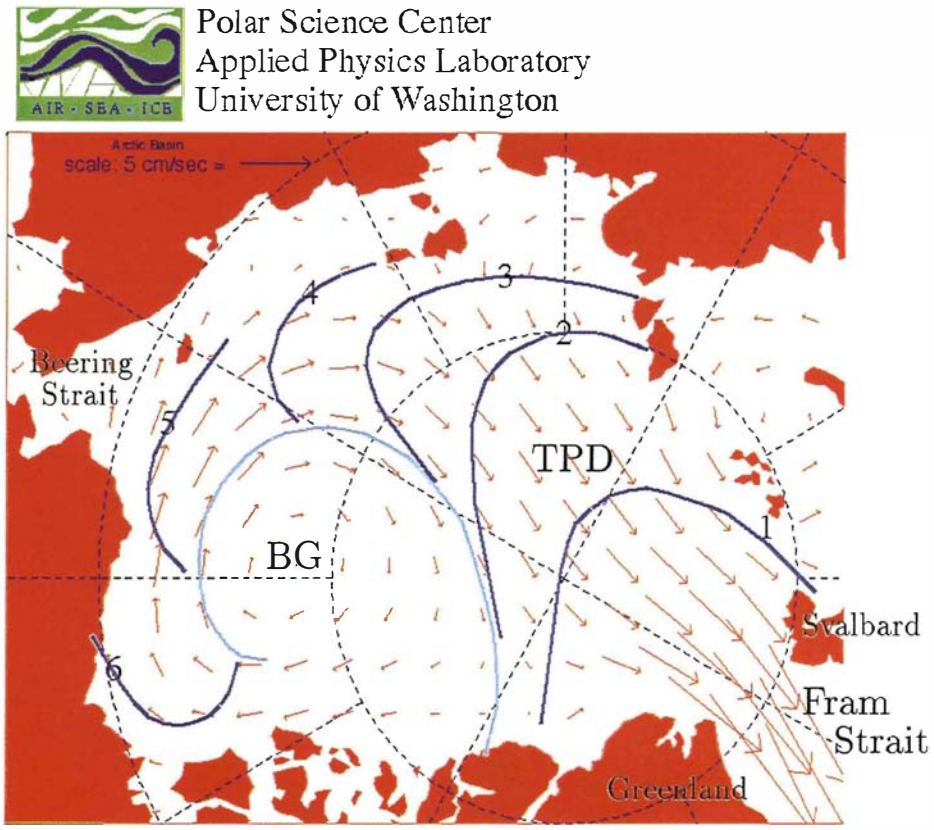

Figure 1.1: Annual mean of ice motion in the Arctic based on 1979-1990 buoy data. The superimposed lines indicate the number of years till the ice exits the arctic basin through the Fram Strait (from International Arctic Buoy Program's World Wide Web pages http://IABP.apl.washington.edu). BG = Beaufort Gyre, TPD = Transpolar Drift Stream.

Arctic Buoy Program, IABP), where the mean annual field of sea-ice motion based on past drifting buoys, ice stations, and beset ships observations is shown (see also Colony & Thorndike 1984 and 1985). The export of ice may be interpreted as the net production of Arctic sea-ice, an important climate signal (Colony & Thorndike 1994; Barry et. al. 1993). This transport of sea ice is also a major source of fresh water and of negative latent heat into the Greenland Sea affecting the circulation of the Northern Atlantic (Aagard & Carmack 1989; Unterstein 1988). Ice flux calculations in Fram Strait can also be related to Arctic conditions (Englebretson & Walsh 1989).

Estimations of ice flux through the Fram Strait serve as effective constrains on model simulations of Arctic climate. To obtain an estimate of the volume flux of sea ice through the Fram Strait, the ice drift velocity and the ice thickness distribution which also includes the ice concentration, must be well known. How the information of velocity and thickness of the ice in the Fram Strait is obtained until now is summarized below. Ice thickness

information from the Fram Strait is based on:

1. upward looking sonar profiles obtained from submarines (Wadhams 1992) (see also Figure 20 in Vinje & Finnekåsa (1986) based on earlier observations reported by Wadhams (1981 and 1983) and Hibler (1980).) These observations show a cross-stream variation from 1–2 meters in the marginal ice zone to 5–6 meters when approaching the Greenland shelf. The mean ice thickness observation in May 1987 also shows a decline in mean ice draft of about 0.34 meters per latitude Wadhams (1992).

2. studies of drilled ice cores and observations of surface features (Vinje & Finnekåsa 1986) which give a fair estimate of the average distribution of ice across the Fram Strait. Along the 81°N-latitude these observations show an ice thickness between 4.4 meters near the coast of Greenland and 2.9 meters at the northern tip of Svalbard during August. From ice cores drilled in the Fram Strait during summer 1984, Tucker et. al. (1987) recorded first year ice thicknesses of between 38 cm and 236 cm and multi year ice thicknesses ranging from 174 cm to 536 cm.

3. upward looking sonars mounted on oceanic moorings provide ice thickness data at a given point for a large period of time (Vinje et. al. 1996; Martin & Lemke 1995). These time series show strong seasonal and interannual variability.

Ice drift information from the Fram Strait is based on:

1. ice velocity data from drifting buoys placed on the ice and drifting with the ice (see results presented in this work) (Moritz 1988; Martin & Lemke 1995; Vinje & Finnekåsa 1986). The locations of the buoys are determined by satellite tracking with adequate precision and sampling rate for resolving the largest features of the field of sea-ice.

2. ice tracking from SAR and AVHRR images from which the drift of single floes can be determined (Sun & Askne 1995; Thomsen et. al. 1995; Korsnes 1994; Aleksandrov & Korsnes 1993; Emery et. al. 1991; Shuchman et. al. 1987; and others). In contrast to the Lagrangian information from a few buoys, remote sensing data provide quasi-Eulerian information on the velocity field of sea ice (Colony & Thorndike 1994).

All the above listed data on the sea ice drift in the Fram Strait are particular realizations of the sea ice velocity and -thickness at a specific moment of time and position in space.

Chapter 2

Ice drift motion

The trajectories of 122 drifting buoys from the International Arctic Buoy Program and from Norsk Polarinstitutt (Vinje & Finnekåsa 1986) and two manned stations (Papanin 1948?; Ostenso & Pew 1968; Vinje & Finnekåsa 1986) are shown in Figure 2.1 for the Fram Strait area. This data sets will be referred to as the IABP and NP data set.

Of all the buoys contained in the IABP data set, only those passing through the Fram Strait are considered in this work, i.e. those passing the 81°N latitude and further south. The International Arctic Buoy Program co-ordinates the systematic deployment of, and data processing for, a substantial number of sea-ice buoys in the Arctic Ocean. The buoy (ice) drift velocities studied in this work are derived from the IABP co-ordinators and those not included in the IABP dataset are from Vinje & Finnekåsa (1986).

2.1 The East Greenland ice drift

All together there are 4224 daily registrations between 81°N and 75°N for the years 1937, 1965 and from 1976 to 1994. Of these 2621 registrations are from April–September (Figure 2.1a), and 1603 from October–March (Figure 2.1b). On the other hand, all together 92 buoys pass the 80°N latitude, of which half are passing in between April and September and half between October and March. Comparing the total number of daily registrations and the number of buoys passing the considered area, the first intuitive estimate is that sea ice moves faster through the Fram Strait during the winter season. This can also be seen directly from Figure 2.1. The buoys seem to move more frequently in eddy structures during summer and more straight forward during winter.

Figure 2.2 shows histograms of the buoy drift velocity for all daily buoy registrations between 81°N and 75°N, and their seasonal means. The drift velocity is presented by the velocity magnitude, v, and velocity direction, α, at the considered position of a buoy registration. Here, α is the angle from the x-axis in a polar stereographic map projection in which the y-axis is parallel with the 32°W-meridian. The azimuth direction (°N=0, °E=90) is given by $\alpha_{az.} = 90° - \alpha + lon + 32°$, where lon is the actual longitude degree.

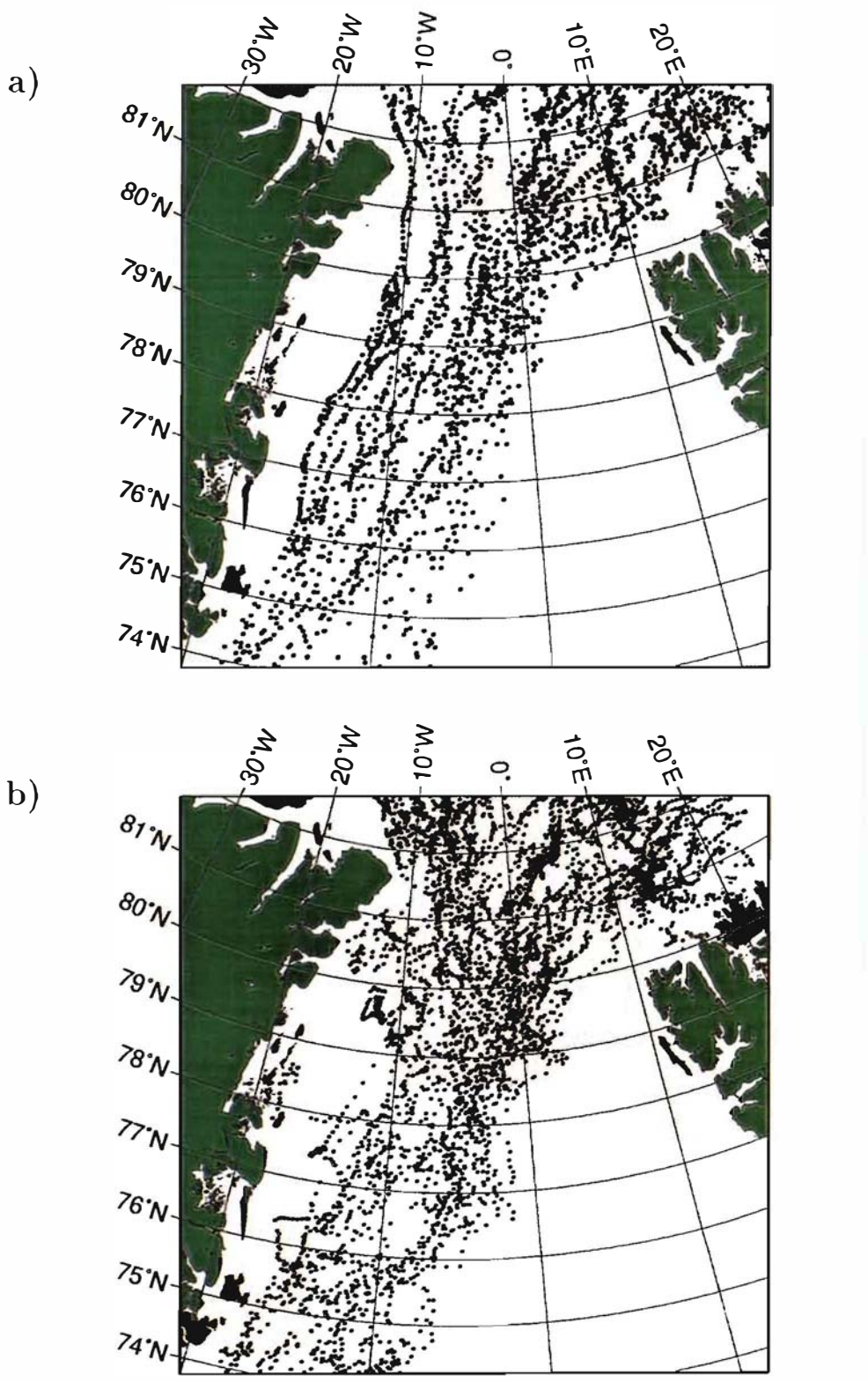

Figure 2.1: Positions of daily registrations of drifting buoys passing through the Fram Strait from 1976 to 1994 between a) April and September and b) October and March.

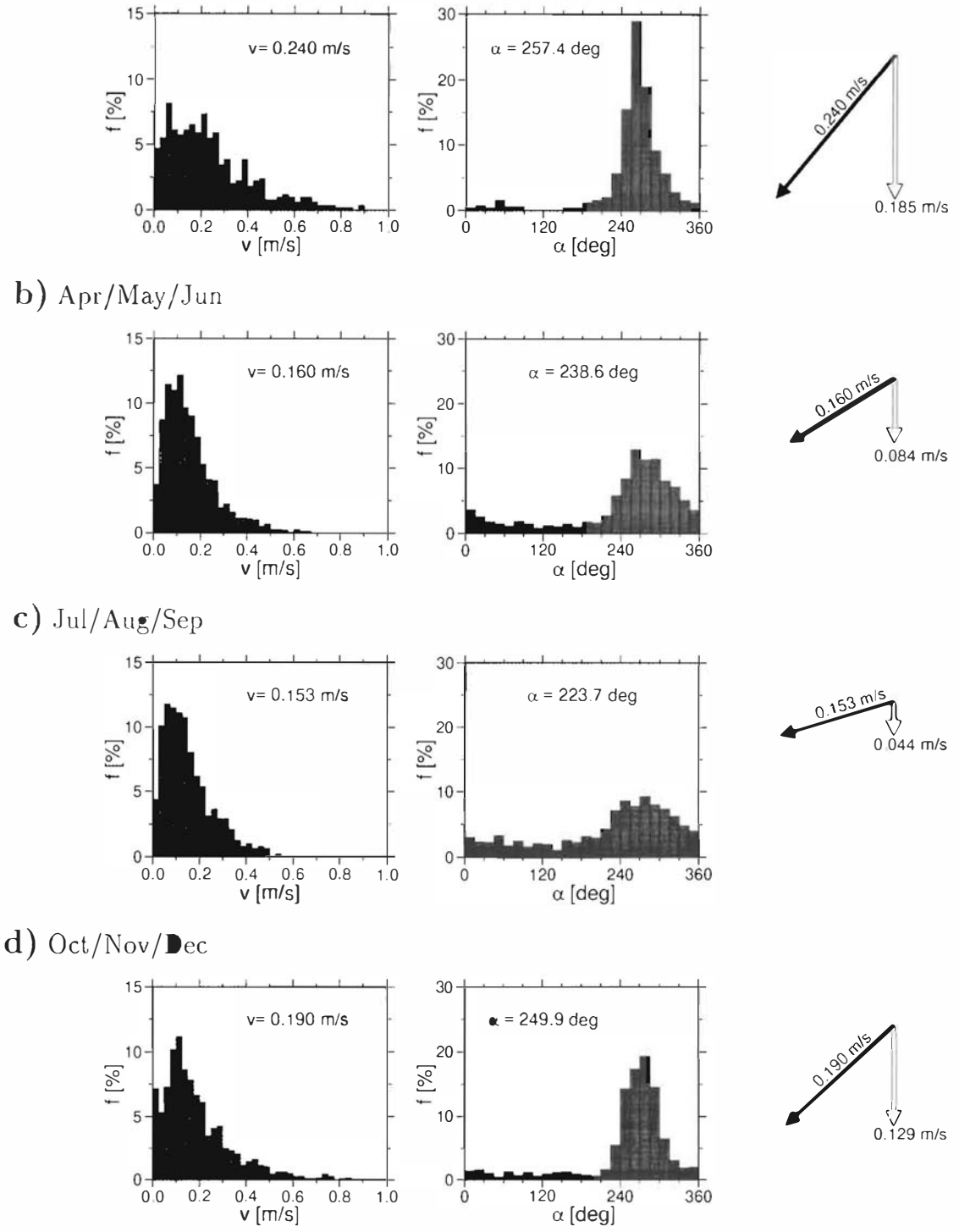

Figure 2.2: Histograms of the buoy drift velocity, magnitude, v, and stereographic direction, α, for all daily registrations between 75°N *and* 81°N and their seasonal mean value specified specially. f is the frequency, i.e. number of registrations given in percent of total number of registrations. With a mean longitude at 5°W, the black arrow represents the seasonal mean buoy velocity with azimuth direction, white arrow represents the seasonal mean South component.

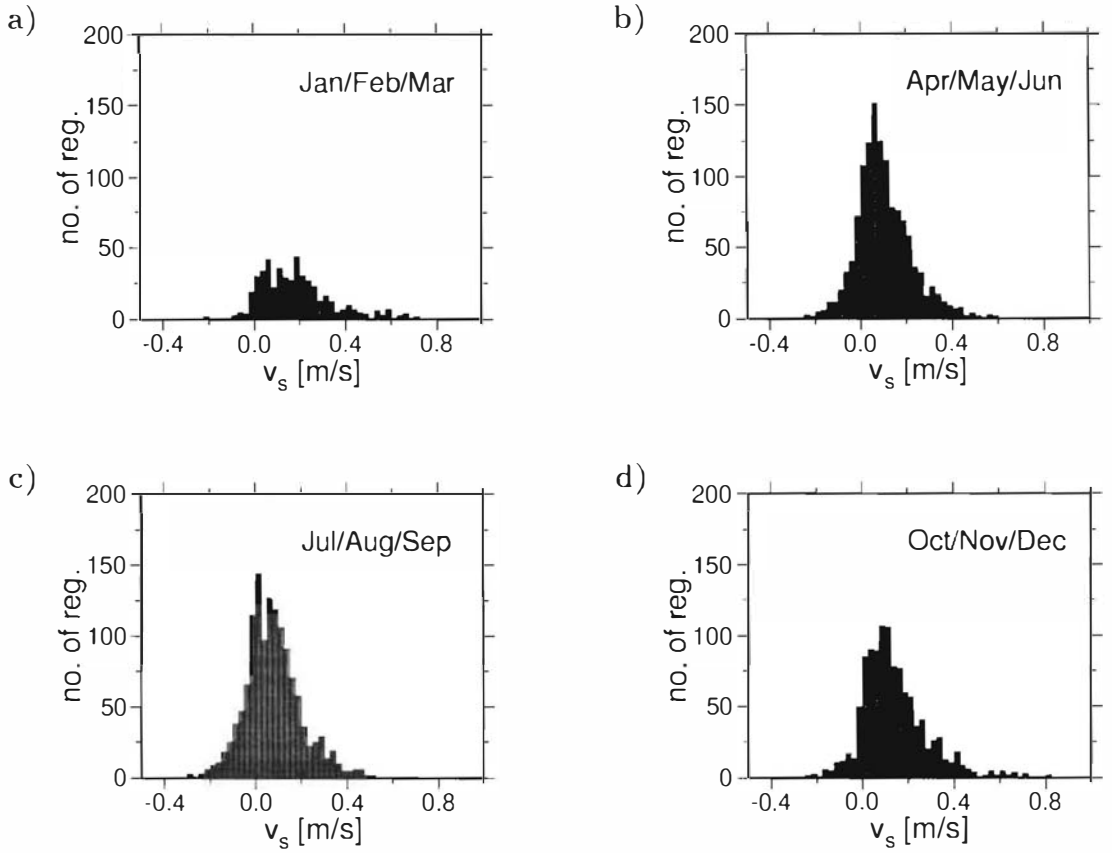

Figure 2.3: Histograms of the South component of the buoy drift velocity for all buoy registrations between 75°N and 81°N. The total number of registrations for the considered period of time is a) 490, b) 1282, c) 1339 and d) 1113.

In Figure 2.3 the South component of the drift velocity at each buoy registration is shown in histograms.

The buoy data show mean velocities up to 0.240 ms^{-1} in the winter months, January–March, of which 75% of the registrations have a direction between α =240 and α =300 degrees and no registrations between α =90 and α =150 degrees (Figure 2.2). In January–March only about 5% have a Northward component (Figure 2.3). This shows a very marked Southwestward ice drift along the continental slope.

During the summer months, July–September, the mean value is reduced to 0.153 ms^{-1} with a more smoothed distribution of direction (Figure 2.2). Even though the preferred drift velocity is still along the continental slope, about one third of the registrations have a northward component (Figure 2.3). The ice drift pattern is more complex and the ice moves in large eddy structures during the summer.

In order to show the clear difference from season to season, the three-monthly mean velocities are presented as vectors in Figure 2.2. The buoys drift more straight Southward the stronger the seasonal mean drift velocity is, and more Westward the weaker the seasonal mean drift velocity is.

Converting the seasonal mean meridional velocity (Figure 2.2) to an average residence time by $t = s/\overline{v}_s$, the residence time is 42, 92, 176 and 60 days for January–March, April–June, July–September and October–March, respectively. In the expression for t, s is the distance between 81°N and 75°N and $\overline{v}_s = |\overline{v}\cos(90° - \overline{\alpha} = lon + 32)|$ is the average south velocity represented as white arrows in Figure 2.2 with a mean longitude degree equal to lon =5°W. The number of daily registrations in the considered three-month periods are 490, 1282 =, 1339 and 1113, respectively, and this is roughly inversely proportional to the average Southward drift velocity (Figure 2.2) and then the averaged residence time of ice in the East Greenland Current.

An overview of the drift velocity in the whole East Greenland Current, between 72°N and 82°N, based on all the daily buoy registrations, is shown in Figure 2.4 and Figure 2.5. A closeup of the drift pattern in the Fram Strait is shown in Figure 2.6. The ice drift pattern in Figure 2.4 and 2.5 are for the periods April–September and October–March, respectively. In Figure 2.6 the two time periods are shown in the same plot. The mean velocity at a position, (lat, lon), is obtained by deriving the mean value of all registrations within the area $(lat \pm 0.25°, lon \pm 0.25°)$. The arrow represents the drift velocity within a box area, with the arrow tail at (lat, lon), and is shown together with the number of daily buoy registrations within a box area in Figure 2.4 and 2.5. A considerable increase of the drift velocity with a marked difference between summer and winter results, occurs in the Fram Strait.

Figure 2.1, showing the daily registrations, Figure 2.2 showing histograms of the ice velocity, and Figure 2.6 showing the horizontal distribution of the ice velocity, all indicate that the ice drift through the Fram Strait is fast and straight forward during winter and slower in a complex eddy structured pattern during summer. These main seasonal drift patterns studied in view of the monthly mean sea level pressure, indicate that the ice motion in the Fram Strait is mainly related to sea level winds during winter and to ocean current during summer. Figure 2.7 shows annual monthly mean sea level pressure distribution in the Arctic for July and January based on data from the years 1979–1990 (IABP). In January (Figure 2.7a) large pressure gradients along East Greenland occur with winds then blowing along the isobars. These gradients are negligible in July (Figure 2.7b).

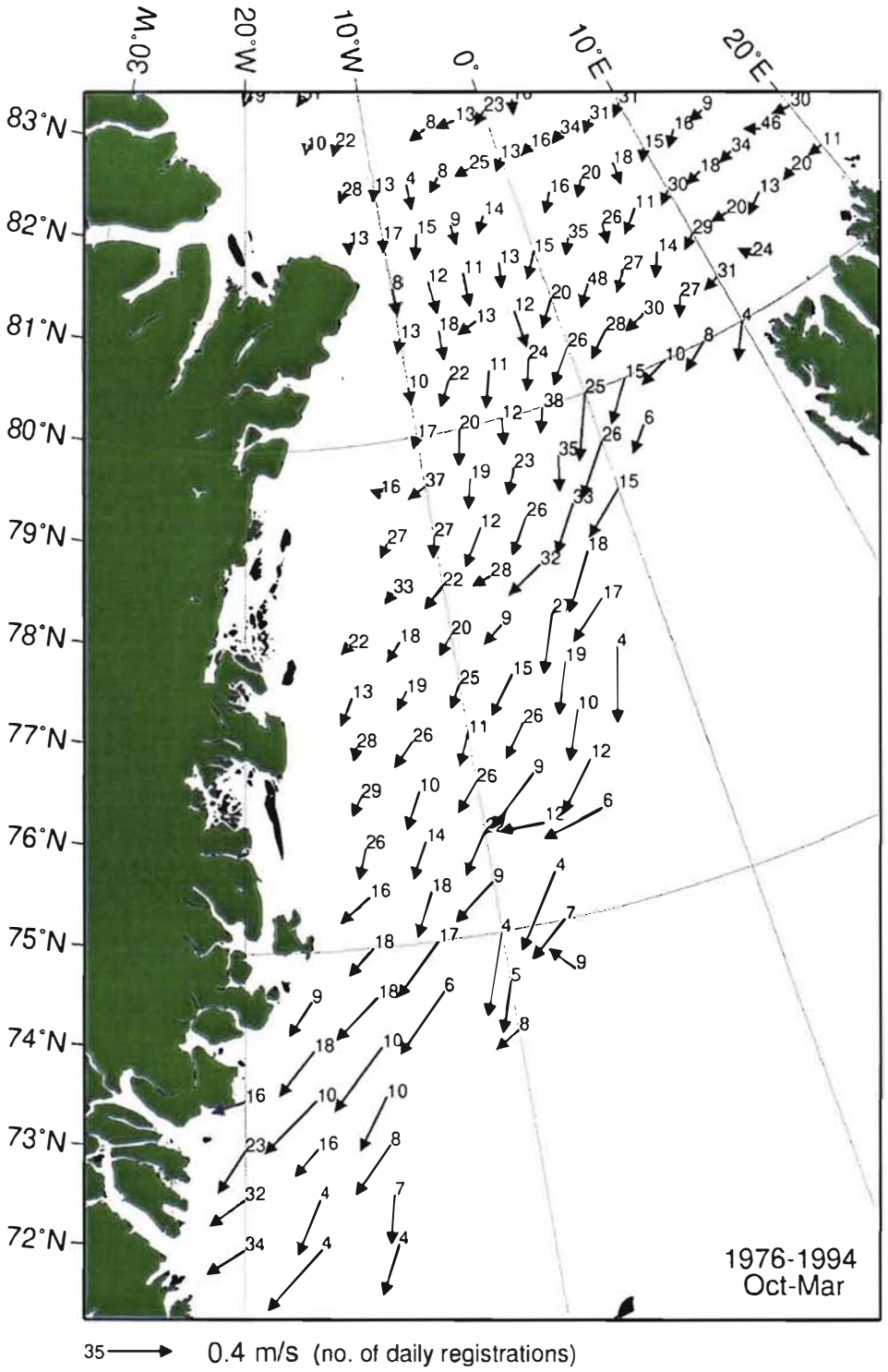

Figure 2.4: Ice drift velocity in the East Greenland Current for buoy registrations between October and March.

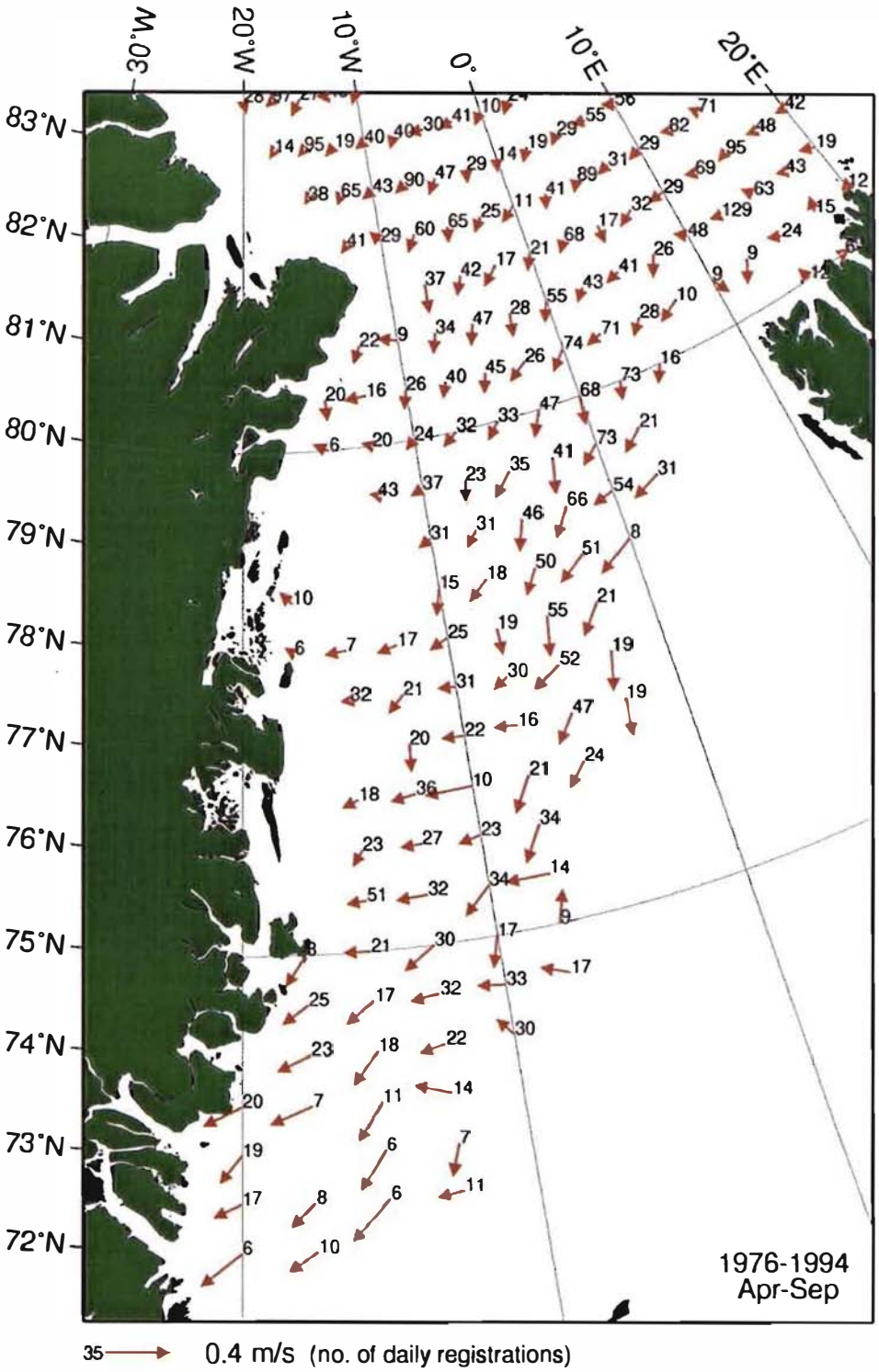

Figure 2.5: Ice drift velocity in the East Greenland Current for buoy registrations between April and September.

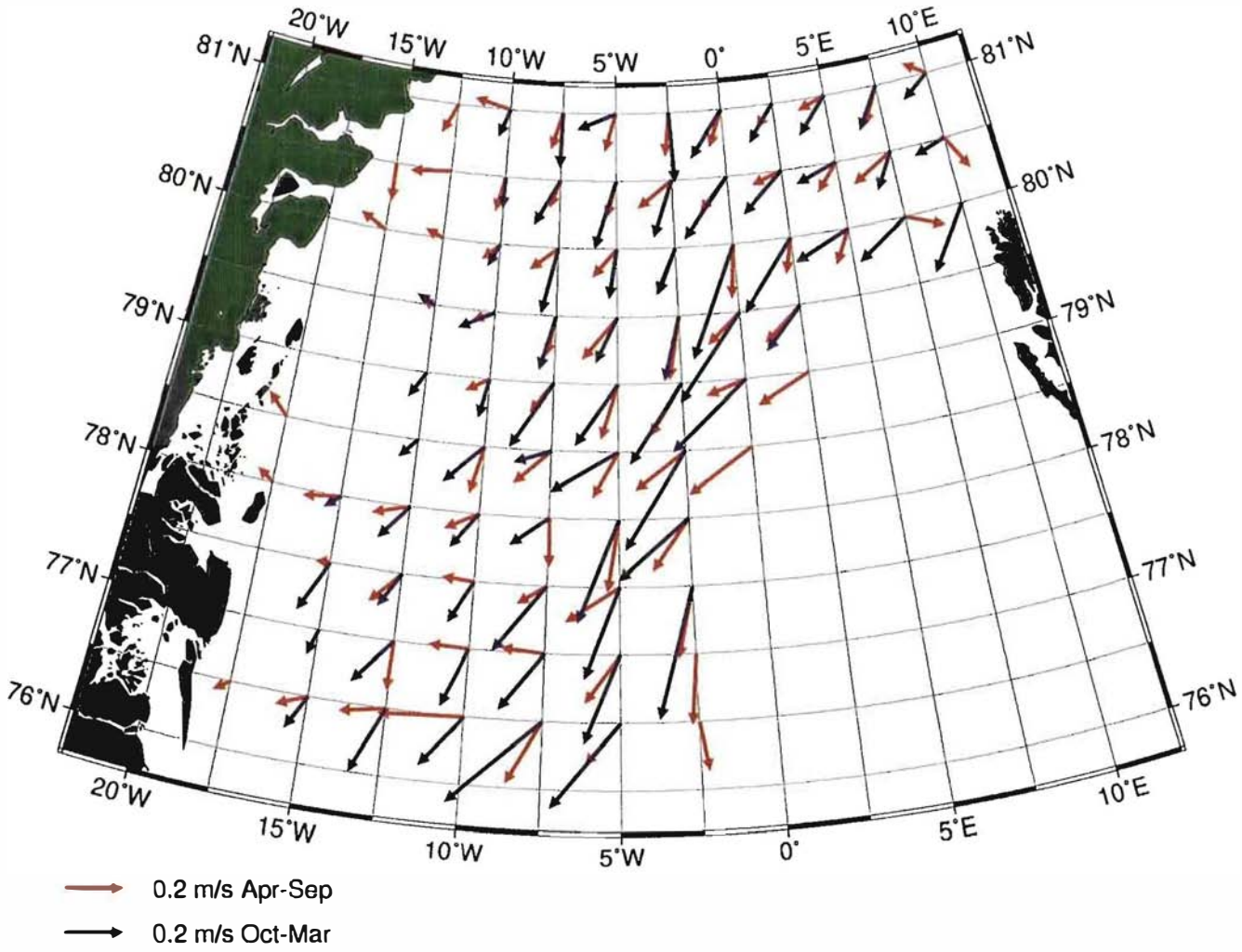

Figure 2.6: Ice drift velocity in the Fram Strait for April–September (Red arrows) and October–March (Blue arrows).

a) January 1979–1990

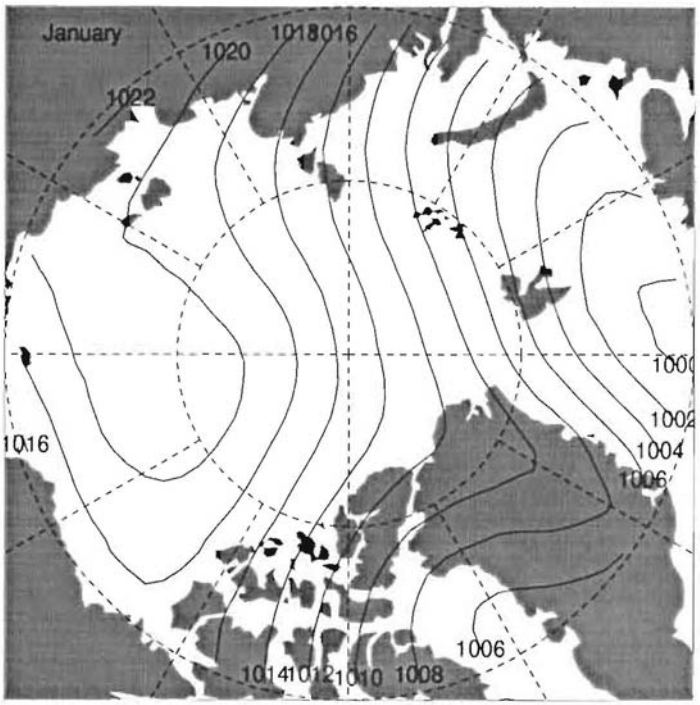

b) July 1979–1990

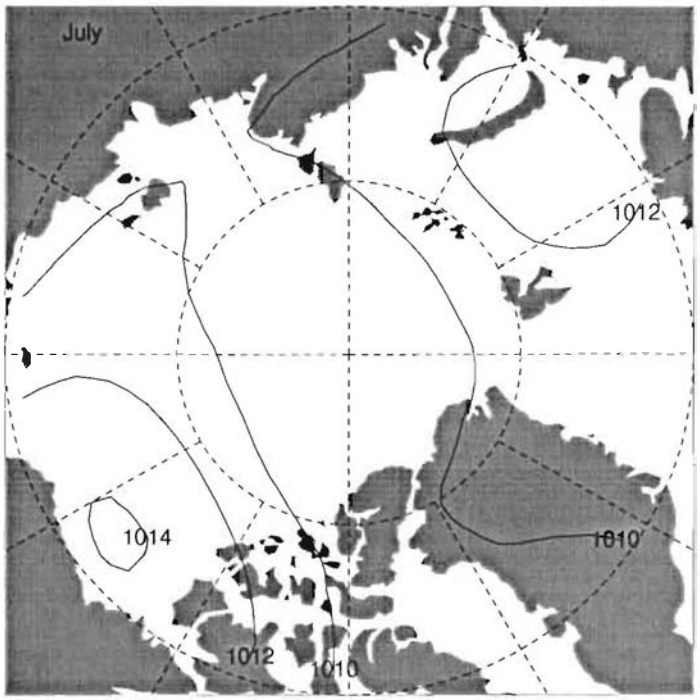

Figure 2.7: Monthly mean pressure (SLP) for a) January and b) July in the Arctic based on data from the years 1979-1990. (Figures from the International Arctic Buoy Program.)

Chapter 3

Ice distribution

From "Navy–NOAA Joint Ice Center Digitized Sea Ice Data", referred to as the NOAA data, the ice concentration is extracted to study the sea ice distribution in the Fram Strait. The NOAA database contains weekly registrations of sea ice from January 1972 to April 1991, covering a total area from about 90°W–90°E and 45°N–90°N. In the Fram Strait area the NOAA data have a resolution of 1° in longitude (East-West) and 0.25° in latitude (South-North).

The ice concentration parameter, C, contains information about the sea ice distribution and sea ice border for a local fraction of an ocean region, but with no information of the sea ice motion or the thickness of the sea ice. That is, the ice concentration shows the horizontal extension and distribution of sea ice in the considered ocean area. Weekly charts of ice concentration over a long period of time give inter annual, inter seasonal and inter monthly variations of the ice cover distribution in an ocean region. C is specified in one-tenth parts (1/10), and the international term given in ice charts from the Norwegian Meteorological Institute have the following classification:

$C =$	1.00	Fast Ice
$C =$	$0.90 - 1.00$	Very close drift ice
$C =$	$0.70 - 0.90$	Close drift ice
$C =$	$0.40 - 0.70$	Open drift ice
$C =$	$0.10 - 0.40$	Very open drift ice
$C =$	$0.10 - 0.00$	Open water
$C =$	0.0	Ice free

where, for example, C =0.90 means that 90% of an ocean region is covered with sea ice. Ice concentration in the Fram Strait area is an important parameter when estimating the sea ice volume flux out from the Arctic Ocean.

In the present work the north part of the Fram Strait is studied, covering a total area of A_{tot} =660,933 km^2, between -25.5°W – 15.5°E and 75.875°N – 82.875°N. Inter seasonal and inter annual variations in the Fram Strait ice distribution during the years 1972–1990,

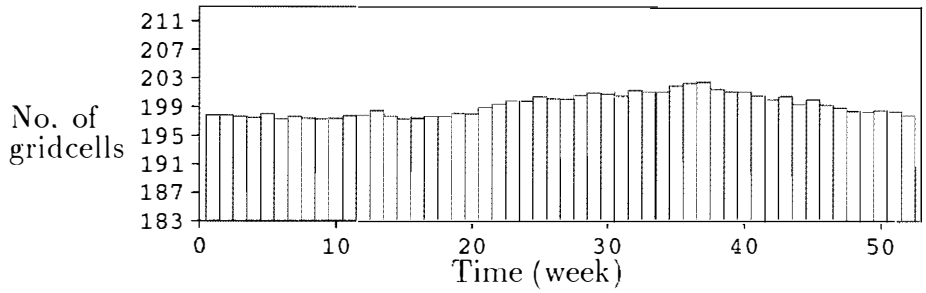

Figure 3.1: Weekly number of gridcells with land-values averaged over the years 1972–1990. Total number of gridcells is 1428.

are presented. In addition to describing the seasonal variations, periods of time with large deviations from the means are presented specially.

3.1 About the NOAA database

In december 1996, Norsk Polarinstitutt received a CD-ROM from the National Snow and Ice Data Center, NSIDC (formely known as Navy/NOAA Joint Ice Center), with reprocessed sea ice data for the period 1972–1991, and new digital sea ice data from 1991–1994. In the documentation following the CD-ROM, (NSIDC: Arctic and Antarctica Sea Ice Data 1996), the identified errors in the old dataset and corrections in the new dataset are specified. In this work the old dataset is used, and changes in the new dataset of importance for this work is commented in connection with the actual subjects.

The NOAA data sources have been shore station reports, ship reports, aerial reconnaissance and satellite imagery and data, where the latter compromise over 90 percent of the data utilized in the Arctic sea ice analyzes from 1972–1990 (Knigth 1984). Today, sea ice analysis is done almost exclusively with remote sensed data. For this sea ice dataset the relative accuracy and level of analysis detail vary over the years, and the utilization of each data type varies both temporally and spatially in the weekly analysis files. For more information about sources, see documentation on the CD-ROM (NSIDC: Arctic and Antarctica Sea Ice Data 1996).

The NOAA data are stored in a standardized format for gridded sea ice information, called SIGRID, established by the World Meteorological Organization Commission for Marine Meteorology (World Meteorological Organization - Commission on Marine Meteorology 1989). The gridpoints are defined to be located in the middle of the gridcells in the SIGRID format. According to old documentation of the NOAA data, it is questionable how the grid is organized in the base. In this work it has been assumed that the gridsystem in the NOAA database were actually originated as defined in the SIGRID format. The SIGRID format has a possibility to store nine categories of parameters. The NOAA data cover parameters dealing with ice concentration, stage of development and form of ice. The

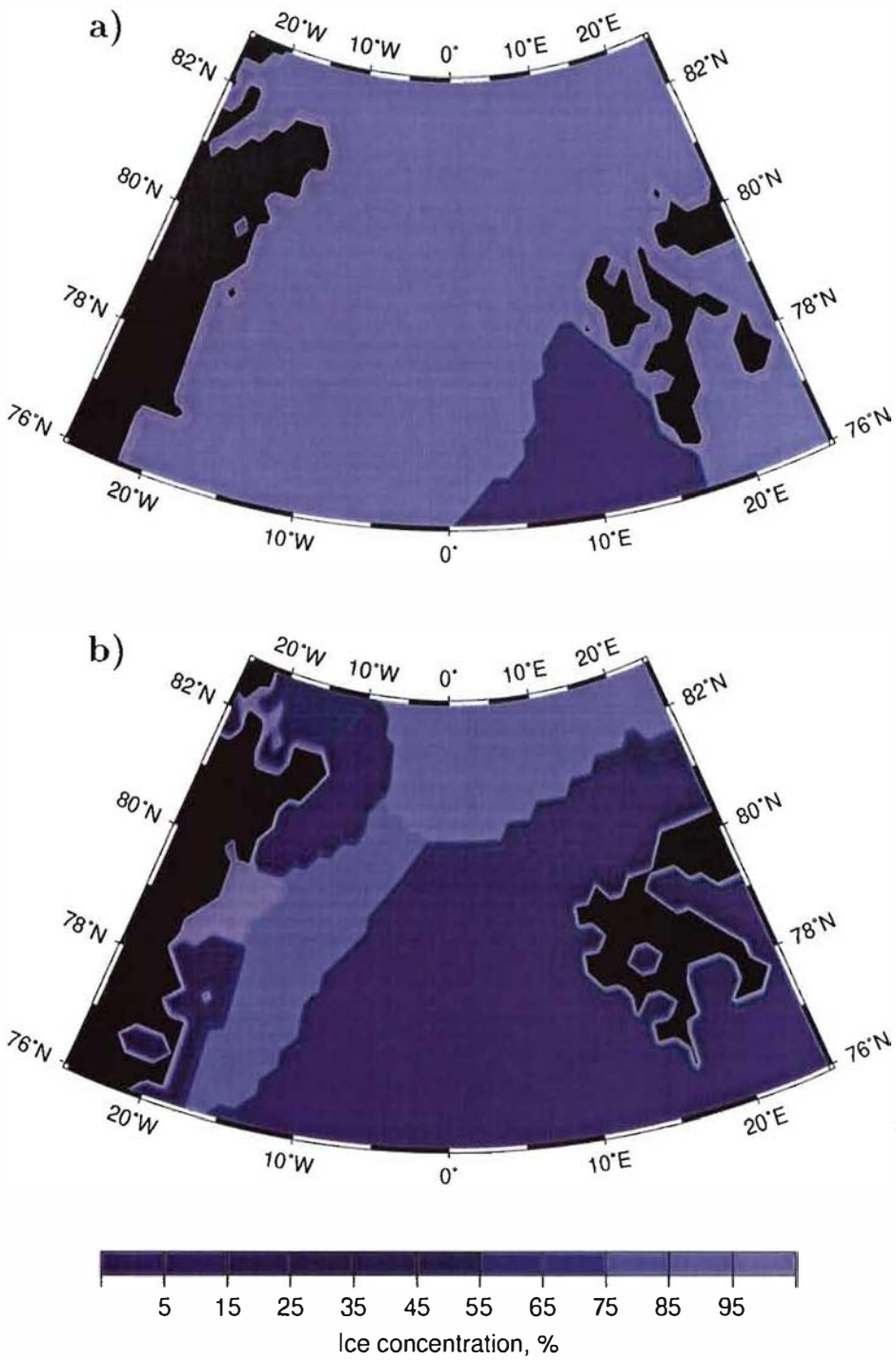

Figure 3.2: Ice concentration in the Fram Strait Area a) on January 3 1972 and b) on September 9 1990. The black color displays the land-points as given in the NOAA data.

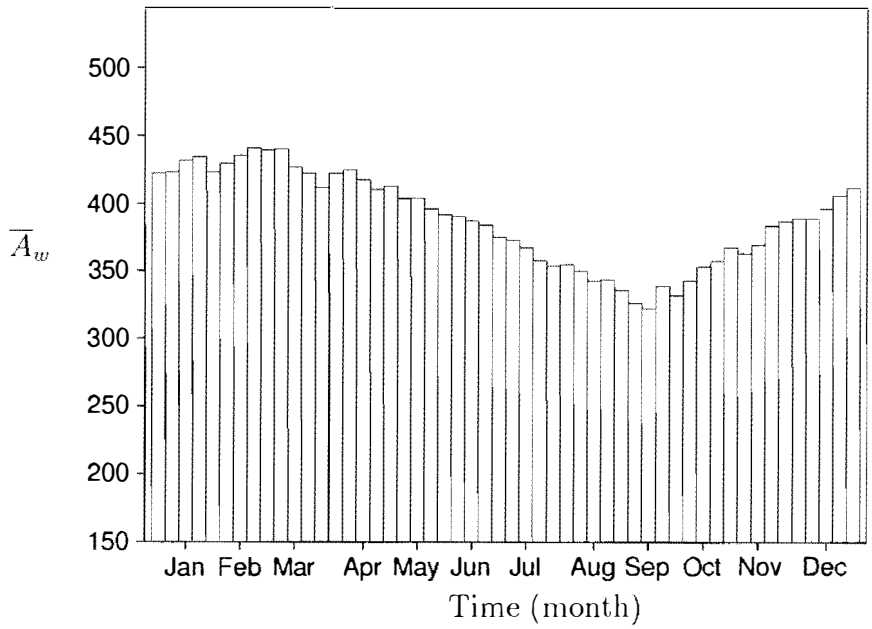

Figure 3.3: Weekly area covered with ice, $\overline{A}_w$ (in 10^3 km^2), averaged over the years 1972–1990.

ice concentration in a NOAA gridcell is specified as intervals, for example 46, which means ice concentration in the interval 0.4–0.6. In this work, mean values will be presented, and ice concentration in the interval 0.4–0,6 will be given the value 0.5. The term Fast Ice is usually understood to be landfast ice, where the sea ice is attached to land. In the old NOAA database an ice concentration equal to 10/10=1 does not necessarily mean Fast Ice, but a gridcell totally covered with ice. When this ice is landfast the matter is specified in another parameter which is not considered in this work.

The number of gridcells with land-values in the old NOAA database varies. For all week registrations during the years 1972–1990, the number of land-points on average increases during the months May–September (Figure 3.1) and during the years 1983-1990. Horizontal distributions of the ice concentration in the Svalbard area tend to show that the fjords are digitized as land-points when they are ice free, and as ice points when they are ice covered, see figure 3.2a. Breitenger (1996) documents inconsistenc in area extent of the Arctic land mask and finds the same variations as presented in this work for the Svalbard - Greenland area. The increase in total land area in 1983 was due to an unaccounted change in map projection. The landmask irregularities were corrected in the new sea ice database (NSIDC: Arctic and Antarctica Sea Ice Data 1996).

In this report, using a computing area between -25.5°W – 15.5°E and 75.875°N – 82.875°N, the number of land-points mainly varies between 199 and 207, except for one registration on October 28, 1975, when the number of landpoints was 214. The main variation is then only 0.8% of the total number of gridpoints, i.e. 1148. The results presented in this work are not corrected for the varying number of landpoints, but special

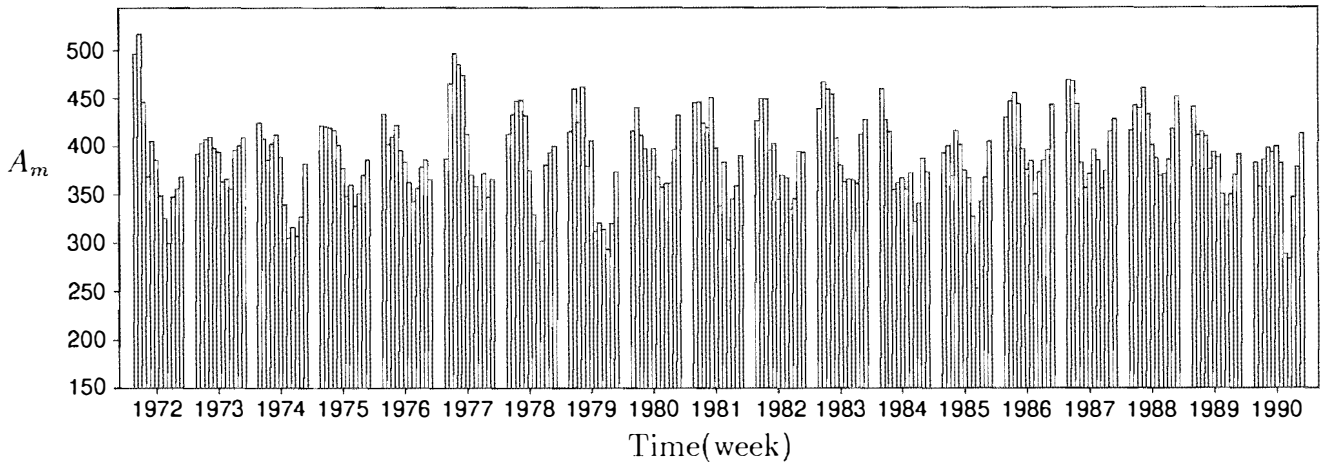

Figure 3.4: Monthly mean value of area covered with ice, A_m (10^3 km^2), for each year 1972 to 1990. To separate each year there are placed three zero columns between each year.

comments is made for the results affected by it.

Both cross-strait profiles and horizontal distributions of ice concentration from the NOAA database have been compared specially with the ice charts from the Norwegian Meteorological Institute for five different years. This comparison shows that the border between ice covered (ice concentration >0) and ice free areas is about the same. The values of ice concentration are somewhat different, but the database and the charts do agree about typical trends in the ice distribution.

3.2 The Fram Strait ice extent

In order to describe the variation of ice cover in the Fram Strait, horizontal distribution of ice concentration values and histograms of various mean values of ice covered areas have been derived. The mean values are defined as:

$$C_j = \sum_{i=1}^{n} C_i/n \quad \text{and} \quad A_j = \sum_{i=1}^{n} A_i/n \tag{3.1}$$

where C_i is the ice concentration given in 1/10 parts for each weekly registration, A_i is ice covered area in km^2 for each weekly registration, and n is the number of weekly registrations included in the mean value.

The j subscript is set to w for weekly registration, A_w, and m for a monthly mean value for one specific year, A_m and C_m. For mean values derived for the whole 1972–1990 period, an overbar is introduced, $\overline{A}_w$, $\overline{A}_m$ and $\overline{C}_m$. The total area covered with ice is calculated by

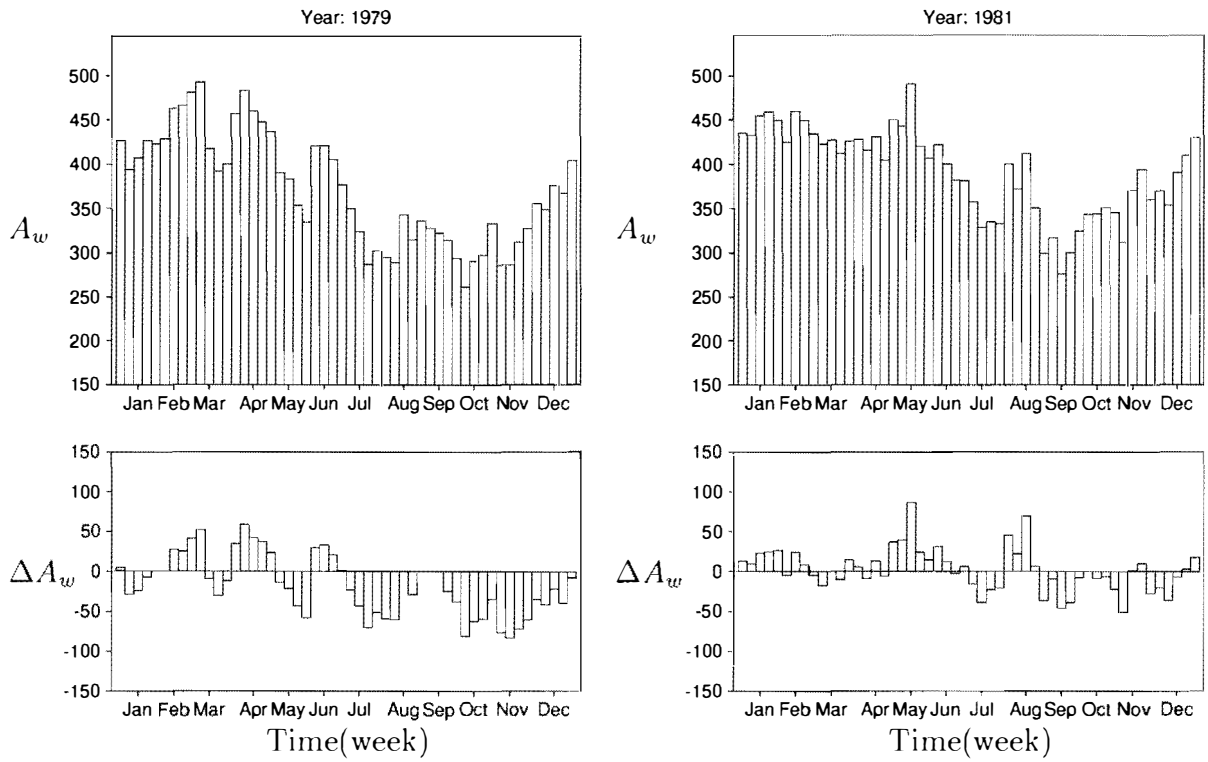

Figure 3.5: Histograms of weekly area covered with ice, A_w (10^3 km^2), and its deviation from the mean, $\Delta A_w = A_w - \overline{A}_w$ (10^3 km^2), for the years 1979 and 1981.

adding the area of all gridcells that have ice concentrations greater than zero, i.e., $C_i > 0$, taken into account that each gridpoint is located in the middle of each gridcell, which area varies with latitude. In the documentation on the new release of the Sea Ice data (NSIDC: Arctic and Antarctica Sea Ice Data 1996), (see chapter 3.1), a considerable error, which is significant for this work, is announced; in most cases in the old database open water (01) was coded as ice free water (00) in the old database. This means that the ice covered area in this report does not include open water areas, since these are defined as ice-free waters.

Both the calculated ice covered area and the total wet area, A_{wet} with no landpoints, i.e., the total possible area that can be covered with sea ice, are affected by the varying number of landpoints (see chapter 3.1). An example which illustrates this is: The total wet area between -25.5°W – 15.5°E and 75.875°N – 82.875°N, on January 3, 1972, is 547,004 km^2 (Figure 3.2a), on September 9, 1990, it is 541,377 km^2 (Figure 3.2b). These two days represent occasions with extremes for number of landpoints, i.e. a minimum of 219, and a maximum of 207. The main variation is then 0.9% of the total computing area, A_{tot} =660,933 km^2. As a comparative value the total possible wet area is set to A_{wet}=545,000 km^2. This value is also used as the maximum area value on the y-axis in figures showing histograms of ice covered areas, (figure 3.3, 3.4, 3.5 and 3.6). The value for the total area, A_{tot}, is also used for comparison since this value is not affected by the varying landpoints.

The weekly mean values of ice covered area, averaged over the years 1972–1990, $\overline{A}_w$, are shown in Figure 3.3. The period with increasing ice cover starts in September/October,

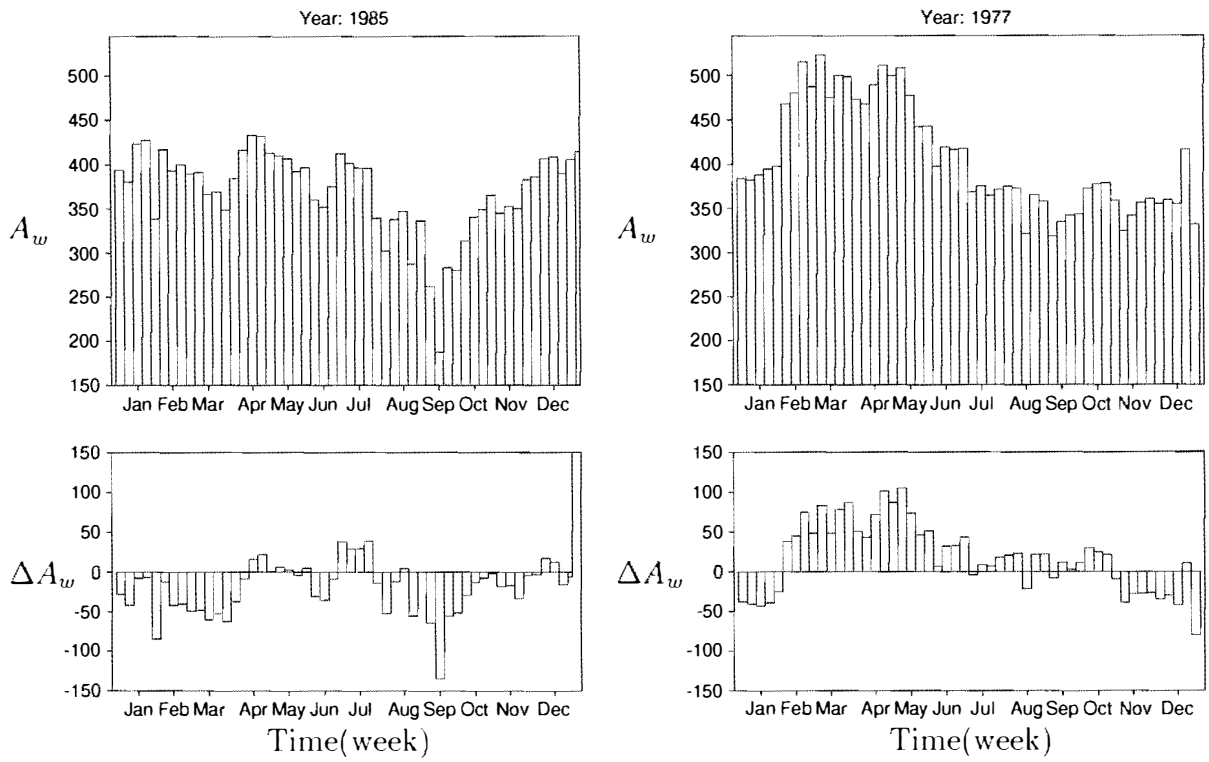

Figure 3.6: Histograms of weekly area covered with ice, A_w (10^3 km^2), and its deviation from the mean, $\Delta A_w = A_w - \overline{A}_w$ (10^3 km^2), for the years 1985 and 1977.

reaching a relatively stable maximum period from late December to March/April. Then the ice covered area decreases to a minimum in September.

In Figure 3.4 monthly mean value for ice covered area, A_m, for each year from 1972 to 1990 are shown. This time series of sea ice extent illustrates the dominant seasonal cycle, which is also seen in the total ice extent in the northern hemisphere (Barry et. al. 1993).

On average, the month of September has least ice extent (Figure 3.3), except in 1974, 1976 and 1986 when the month of August had the minimum ice cover, and in 1979 when the minimum ice extent occurred in October (Figure 3.4). For the considered time period, late February and early March have the largest ice extent (Figure 3.3), with inter annual occurrence of maximum ice covered area between January and April (Figure 3.4). The year 1981 is a special year with maximum ice cover in May ($\overline{A}_m$=568,601 km^2). See also Figure 3.5 which displays the week-values of ice covered area in 1981 and its deviation from the mean. The year 1979 is another special year in the time period where the ice extent increases and decreases within a season, see Figure 3.5 which displays the week-values of ice covered area for 1979.

September 1985 is the month with absolute minimum ice extent in the considered time period, i.e. A_m=253,159 km^2, which is 46.5% of A_{wet}, and 38.3% of A_{tot}. Figure 3.6, which displays the week values for ice covered area in 1985, shows that there was very little ice in the area this year. In particular, the registration on September 10, 1985, contains the absolute minimum value for ice covered area during the period from 1972 to 1990, A_w=187,209 km^2. The mean value for September 1990 is the next minimum value of area

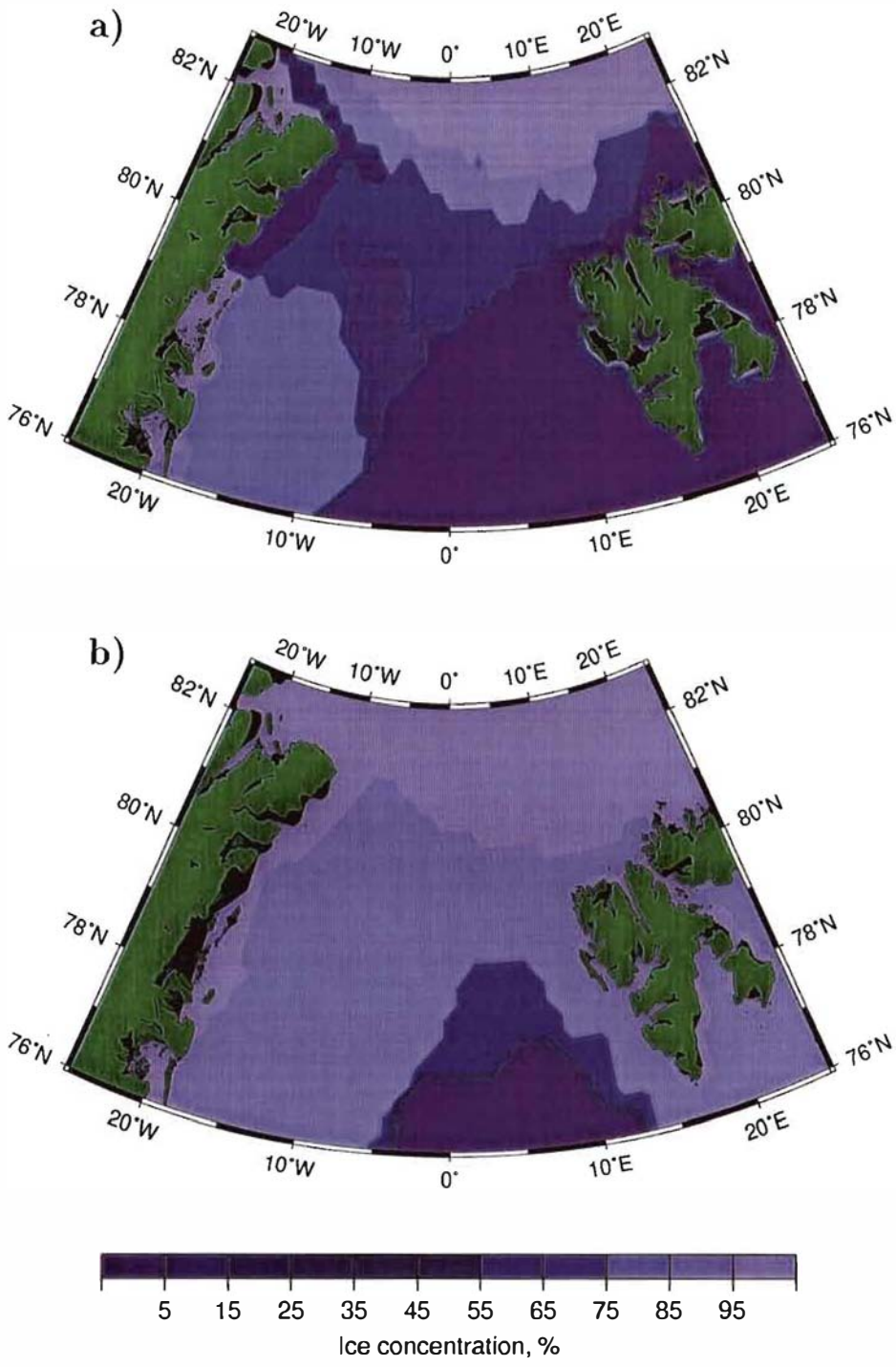

Figure 3.7: Ice concentration in the Fram Strait area a) on September 18 1984 and b) on April 19 1977. The black colour displays the landpoints as given in the NOAA data and the green colour displays actual land area.

covered with ice, A_m=283,445 km^2, i.e. 52.0% of A_{wet}. Figure 3.2b displays the horizontal distribution of ice on September 5, 1990. Figure 3.7b shows the ice distribution on September 18 1984, where A_w=339,387 km^2, which is only 62.3% of A_{wet}. The ice extent is small and the distribution is somewhat different, showing the coastal polynya south of Nordostrundingen on Greenland and also open water north of Nordostrundingen. In Vinje & Finnekåsa (1986), special features like this polynya, are described and confirmed with NOAA satellite images.

February 1972 is the month with absolute maximum ice extent during the years from 1972 to 1990, (Figure 3.4), with $\overline{A}_m$=517,535 km^2 which is 95.0% of A_{wet} and 78.3% of A_{tot}. February–March 1972 is also the period of time during all the years from 1953 to 1990, when the Arctic sea ice extent was at a maximum (Barry et. al. 1993). In March 1977 the next maximum value occurs, A_m=496,866 km^2, i.e. 91.2% and 75.2% of A_{wet} and A_{tot}, respectively. Figure 3.6 displays the week values of ice covered area in the year 1977 and its deviation from the mean value. As an example of ice distribution in the Fram Strait at times with large ice cover, Figure 3.2a displays the ice distribution on January 3, 1972, where A_w=473,389 km^2, 86.7% of A_{wet}. Figure 3.7a displays the situation on April 19, 1977, where A_w=489,114 km^2, that is 89.7% of A_{wet}.

Chapter 4

Cross-strait profiles

Cross-strait profiles of ice velocity, ice concentration and width of ice stream are derived in this chapter. These parameters are important contributions together with sea ice thickness observations in order to improve volume flux estimates. Some of the results obtained, are used in volume flux estimates by Vinje et. al. (1996). Volume flux estimates of sea ice through the Fram Strait serve as an effective constraint in model simulations of Arctic climate.

Histograms of where the buoys prefer to go, cross-strait profiles of sea ice velocity and concentration, and ice velocity, geostrophic wind and ice concentration values at actual buoy positions along the latitudes that cross the Fram Strait, will be presented.

Figure 4.1 shows histograms of where the buoys pass different latitudes on their way south through the Fram Strait, together with the bottom topography in meters below sea level. The longitude degree where a buoy passed the considered latitude, is obtained by linear interpolation between the two daily registrations on each side of the latitude the first time the buoy passed it. Figure 4.1 clearly shows that the majority of the buoys drift along the continental slope, that is, the ice clearly follows the topographically trapped current of polar water along the coast of East Greenland (The East Greenland Current). It could be said that the Fram Strait acts like a funnel, a peak concentration of buoys passed between 3–6°W at the 78°N latitude, that is, 41 out of totally 67 buoys. The shaded parts of the histograms in Figure 4.1 represent the buoys passing the considered latitude between October and March. In October–March the widths of the area where the majority of the buoys are passing is 20.3°, 12.6°, 14.9° and 13.3° longitude along 80°, 79°, 78° and 77° North, which are 393.4km, 278.7km, 346.9km and 335.6km, respectively. The winter distribution also indicates two peaks, one around 10°W and one somewhat larger between 0–5°W. This two-peak distribution is somewhat clearer when we look at all the buoys, and will below be related to the cross-strait velocity profile. In April–September there is one narrow peak moving slightly westward from 0° at 80°N to 5°W at 78°N. In April-September the widths of the area where the majority of the buoys are passing are 12.7°, 8.7°, 4.8° and 11.6° longitude along 80°, 79°, 78° and 77° North, which are 246.8km, 185.5km, 111.7km and 292.7km, respectively. The width of the area where the majority of the buoys are passing, is about 1.5 times wider in October–March than in April–September.

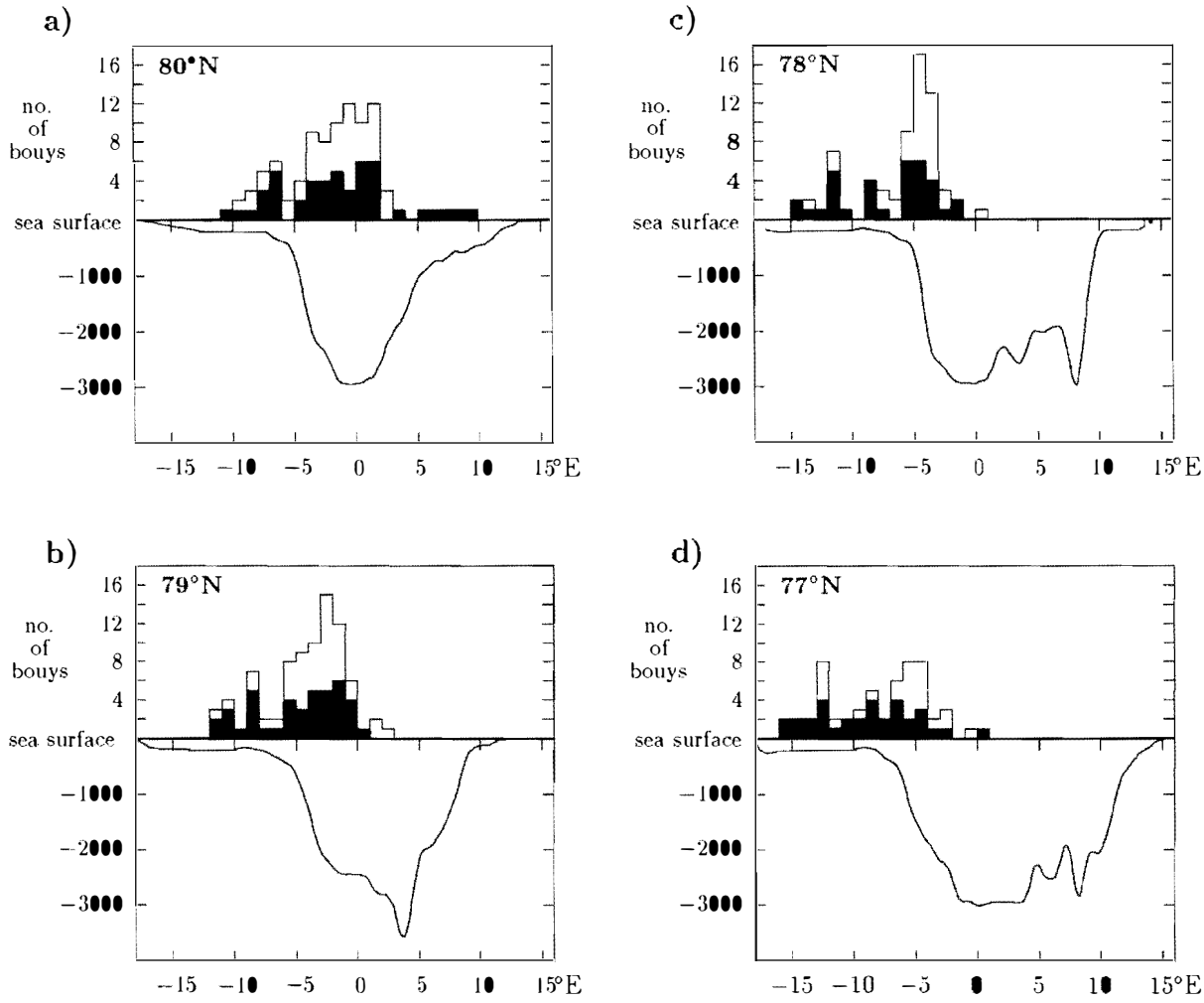

Figure 4.1: Number of buoys passing latitude a) 80°N, b) 79°N, c) 78°N, and d) 77°N in the Fram Strait. Below the line which marks the sea surface, the bottom topography in meters below sea level is shown. The shaded part of the histograms shows the buoys passing between March and October.

The average drift speed profile (averaged over a longitude interval of 5°) at 81°N is given in Table 4.1. The drift velocities are derived in two different ways: First (Table 4.1a) an 'instantaneous' value where the drift velocities are derived from the speed a buoy had first time it passed the considered latitude; second (Table 4.1b) a both space and time averaged value, where the drift velocities from all the daily buoy registrations between 80.5°N and 81.5°N are averaged. The results from the longitudal interval 10°–15°W will hopefully give us a better understanding of what these two mean values represent; there was only one buoy that passed west of 10°W during April–September with 56 daily registrations and with an averaged velocity of 2.3cms^{-1}, i.e. a nearly two-monthly mean drift velocity in the considered area between 10°–15°W and 80.5°N – 81.5°N. On the other hand, the instantaneous averaged value is, in this example, a one time event of a buoy passing 81°N with a velocity of 15.1cms^{-1}. For comparison, the space and time averaged value of October–March west of 10°W represents an about two-weekly mean velocity, while again

Table 4.1: Cross-strait variation of the meridional (South) component of ice velocity (cm/s) across the 81°N latitude. Drift velocities derived a) from the first time a buoy passes 81°N, and b) from all the daily registrations between 80.5°N and 81.5°N and c) comparative drift velocities from Vinje & Finnekåsa (1986) .

	°West			°East			
Period	15–10	10–5	5–0	0–5	5–10	10–15	15–20
a) Apr–Sep	15.1 (1)	15.5 (9)	16.2 (15)	12.3 (7)	11.6 (7)	13.8 (8)	6.5 (2)
Oct–Mar	5.9 (1)	19.8 (8)	20.0 (8)	14.2 (16)	16.1 (4)	9.1 (7)	-
May–Aug	15.1 (1)	16.0 (8)	10.9 (7)	12.3 (7)	15.9 (3)	12.3 (4)	5.8 (1)
Sep–Apr	5.9 (1)	18.9 (9)	20.4 (16)	14.2 (16)	12.2 (8)	11.3 (11)	7.2 (1)
b) Apr–Sep	2.3 (56)	9.5 (131)	9.3 (150)	6.3 (189)	5.7 (135)	3.0 (297)	0.5 (160)
Oct–Mar	8.9 (16)	18.2 (44)	16.1 (68)	12.2 (153)	9.0 (87)	6.6 (88)	3.9 (87)
May–Aug	-0.6 (45)	9.4 (119)	7.5 (101)	5.8 (161)	4.8 (79)	2.2 (220)	0.2 (120)
Sep–Apr	10.9 (27)	16.7 (56)	14.9 (117)	11.7 (181)	8.2 (143)	5.9 (165)	3.1 (127)
c) May–Aug	-	8.1	6.6	6.5	5.4	2.0	1.8
Sep–Apr	-	16.0	12.7	14.9	6.9	9.8	3.6

Number in parenthesis are number of a) buoys passing and b) registrations.

the instantaneous value here represent one buoy passing 81°N for the first time. As a whole, the April–September space and time averaged values are means derived over a longer period of drifting time than the October–March mean values.

The instantaneous averaged value is three times larger than the space and time averaged value in the period April–September between 15°W and 15°E at 81°N, and 1.2 times larger in October–March. These deviations between the two mean values increase when changing the summer season to May–August and the winter season to September–April.

Vinje & Finnekåsa (1986) derived cross-strait drift profiles for May–August and September–April. Compared to Vinje & Finnekåsa's results, the meridional velocity presented here (Table 4.1b) increases on an average by 2.2cms^{-1} and 1.6cms^{-1} west of the 0°-meridian and decreases by 1.4cms^{-1} and 2.6cms^{-1} east of the 0°-meridian for May–August and September–April, respectively.

In Table 4.2 a) the cross-strait variations of the meridional velocity are presented across the latitudes 80°N, 79°N, and 78°N, where the velocities are derived by use of the instantaneous mean values defined above. The cross-strait mean velocity is also presented, and it increases with decreasing latitude. In Table 4.2 b) the drift velocities across 79°N are derived from all daily registrations between 78.7°N and 79.3°N. The instantaneous ice velocity is 2.2 and 1.9 times larger than the space and time mean velocity in April–September and October–March, respectively.

Table 4.2: Cross-strait variation of the meridional (South) component of ice velocity (cm/s). Drift velocities derived a) from the first time a buoy passes 80°N, 79°N and 78°N, and b) from all the daily registrations between 78.7°N and 79.3°N.

		°West			°East		Mean
	Period	15–10	10–5	5–0	0–5	5–10	value
a) 80°N	Apr-Sep	-	16.9 (8)	20.4 (25)	22.7 (13)	-	20.4 (46)
	Oct-Mar	9.9 (1)	24.4 (10)	26.7 (18)	39.6 (13)	20.4 (4)	28.9 (46)
79°N	Apr-Sep	16.3 (2)	18.3 (7)	20.5 (29)	28.7 (3)	-	20.5 (41)
	Oct-Mar	17.2 (5)	22.3 (12)	39.5 (24)	19.1 (1)	-	30.9 (42)
78°N	Apr-Sep	11.1 (3)	16.5 (7)	34.5 (22)	-	-	28.4 (32)
	Oct-Mar	14.0 (10)	28.3 (11)	47.8 (13)	25.7 (1)	-	31.4 (35)
b) 79°N	Apr-Sep	3.6 (28)	8.2 (74)	13.3 (136)	4.7 (68)	-	9.3 (306)
	Oct-Mar	5.9 (58)	15.9 (45)	26.4 (64)	11.0 (6)	-	16.3 (173)

Number in parenthesis are number of a) buoys passing and b) registrations.

If we increase the resolution of the cross-strait ice drift velocity profile from 5° to 2.5° longitudal intervals, we will find a different distribution of ice velocity across the strait during winter. The southward velocity profile in October–March has two extremes (Figure 4.2 solid line) for the profile along 79°N. These two extremes are located between 7.5°–10°W and between 0–5°W, which is fairly well correlated to the two–peak histogram distribution of where the buoys pass this latitude (Figure 4.1). These two winter extremes can be seen in almost all the cross-strait velocity profiles between 76°–81°N (Figure 2.6). In April–September there is one extreme velocity value located between 2.5°–5°W, with a velocity value lower than each of the two winter extremes.

Cross-strait profiles of ice concentration from the NOAA-data along 79°N have also been studied more closely. The longest period of time when the Fram Strait was totally ice covered along 79°N during the years 1972–1990, was from February to the end of May in 1977. Also from January to March 1972 the Strait was totally ice covered along 79°N. There were also quite high ice concentration values along 79°N from February to March 1986. Other years also have no open water along 79°N, but not for such long periods of time and not with such high ice concentration values as reported above. Examples of cross-strait ice concentration profiles along 79.0°N are shown in Figure 4.3. This figure shows the monthly mean ice concentration in April 1977 and April 1984, situations with large and small ice cover extent. For comparison, the mean ice concentration in April averaged over the years 1972–1990, is shown. The conclution is that the Fram Strait is rarely totally ice covered in April along 79.0°N.

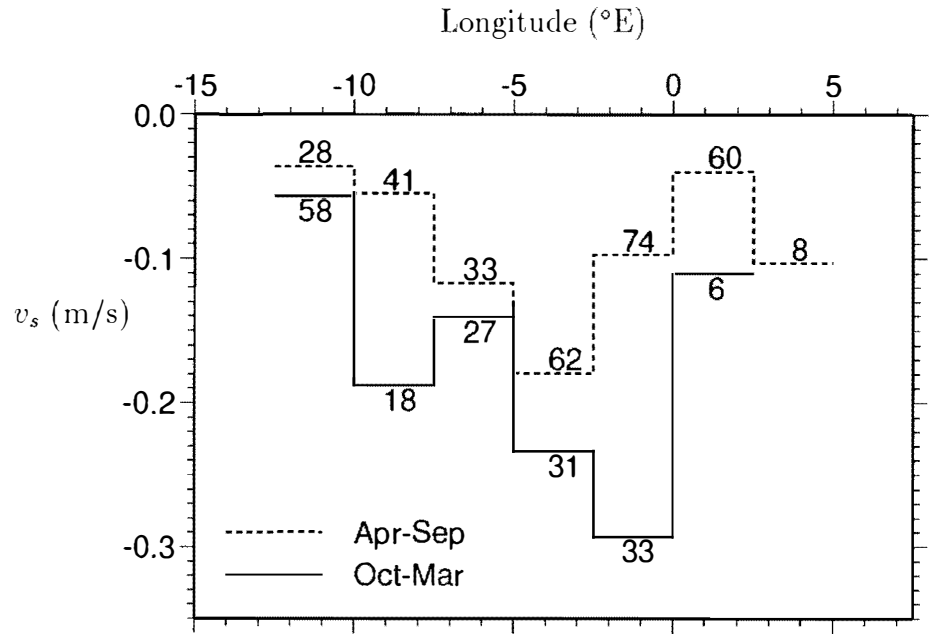

Figure 4.2: The cross-strait velocity profile (South component) derived from all daily positions between 78.7° and 79.3°N in the Fram Strait, for April–September and October–March. The numbers represent the number of daily registrations in the considered longitudal interval.

4.1 Registrations at the actual buoy positions

The ice drift velocity ($\diamond$), and the geostrophic wind (+), for each buoy when passing the latitudes 80°N, 79°N and 78°N in the Fram Strait are shown in Figures 4.4, 4.5 and 4.6. The magnitude is shown in Figure a), and the direction with the x-axis normal to the 32°W-meridian in a polar stereographic map projection is shown in Figure b). The cross-strait mean values of ice velocity, v, and geostrophic wind, w, are also given explicitly in Figure a), and the cross-strait mean angle between the wind and ice velocity vectors, $\alpha_{(w-v)}$, is given explicitly in Figure b). The ice concentration, i.e., the local fraction of the ocean area covered with sea ice, in the neighborhood of each buoy, is presented in Figures 4.4c, 4.5c and 4.6c when the buoys passed the latitudes 80°N, 79°N and 78°N.

The ice drift velocity is derived from the IABP and NP drifting buoy data set and calculated by linear interpolation on the polar stereographic map projection, between the drift velocities of the two daily registrations on either side of the considered latitudes. Linear interpolation of the corresponding positions give the longitude degree where the buoy passed the considered latitudes (see also Figure 4.1).

In order to avoid assumptions on details in the sea ice surface boundary layer, we choose to present the geostrophic wind together with the ice drift velocities. The geostrophic wind is derived from the hindcast wind dataset from the Norwegian Meteorological Institute, which contains four sea level wind fields (10 meters above sea level) per day on the polar stereographic map projection with 75 km grid resolution. The wind vector at a buoy position is obtained by bilinear interpolation in the hindcast datagrid. The sea level wind is converted to geostrophic wind with magnitude and direction factors also from the Norwegian Meteorological Institute. The daily mean wind values on the day the buoy passed the

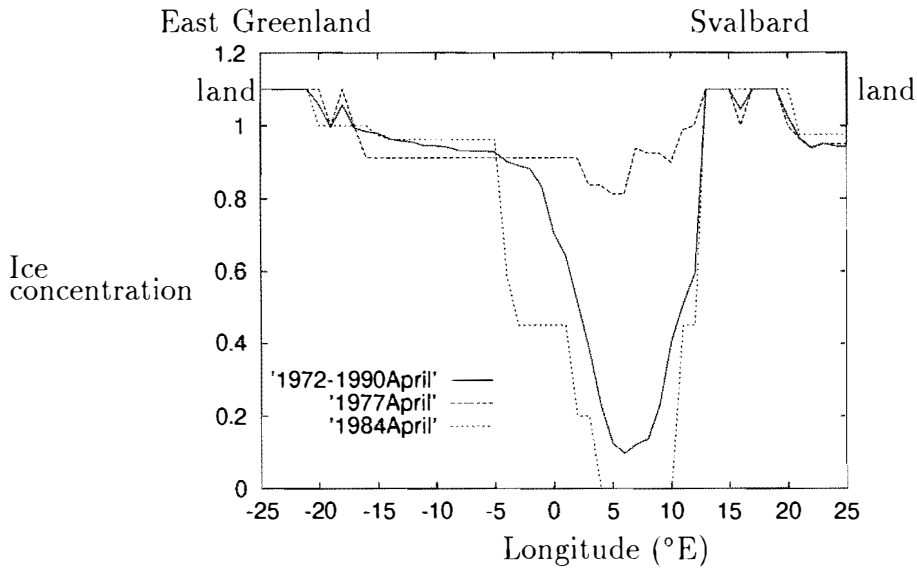

Figure 4.3: Cross-strait profile of monthly ice concentration, C_m, in April 1977 and 1984, and mean value, $\overline{C}_m$, for April averaged over the years 1972–1990 at 79°N.

considered latitude are presented on the plots.

The ice concentration data are from the NOAA data, which contain weekly ice concentration fields with a resolution in the Fram Strait area of 1° in an East-West and 0.25° in a North-South direction, as described previously. The ice concentration values presented in Figure 4.4–4.6c are obtained by first finding the gridcells in which each buoy position is located. The weekly value of ice concentration the this gridcells is then found for the registration date closest to the day the buoy passed the considered latitude. That is, the presented ice concentration values are from maximum 3–4 days from the actual days the buoys passed the considered latitudes. This can be the reason why some buoy registrations have an ice concentration value corresponding to ice free areas.

The wind drag on the sea ice surface may vary considerably from floe to floe in an ice field, and this may cause more or less individual ice floe movements, as observed by Vinje (1977). And as stressed by Vinje & Finnekåsa (1986) such individual ice floe movements should be kept in mind when wind effects on ice motion is investigated.

Averaged over the three latitudes of consideration, i.e., 80°N, 79°N and 78°N, the cross-strait mean ice velocity and wind magnitude are, respectively, 1.4 and 1.8 times larger during April–September than during October–March. And the wind magnitude is about 30 and 40 times larger than the ice velocity in April–September and October–March, respectively (Figure 4.4–4.6a). The increase in ice velocity during the winter season can be related to the increase in geostrophic wind.

The cross-strait mean angle between the wind and the ice velocity is somewhat larger in April–September ($\approx 20°$) than in October–March ($\approx 10°$) (Figure 4.4–4.6b).

On average, the area around the buoys has slightly lower ice concentration in April–September (≈ 0.85 close drift ice) than in October–March (≈ 0.90 very close/close drift ice), when the zero ice concentration values are not included (Figure 4.4–4.6c).

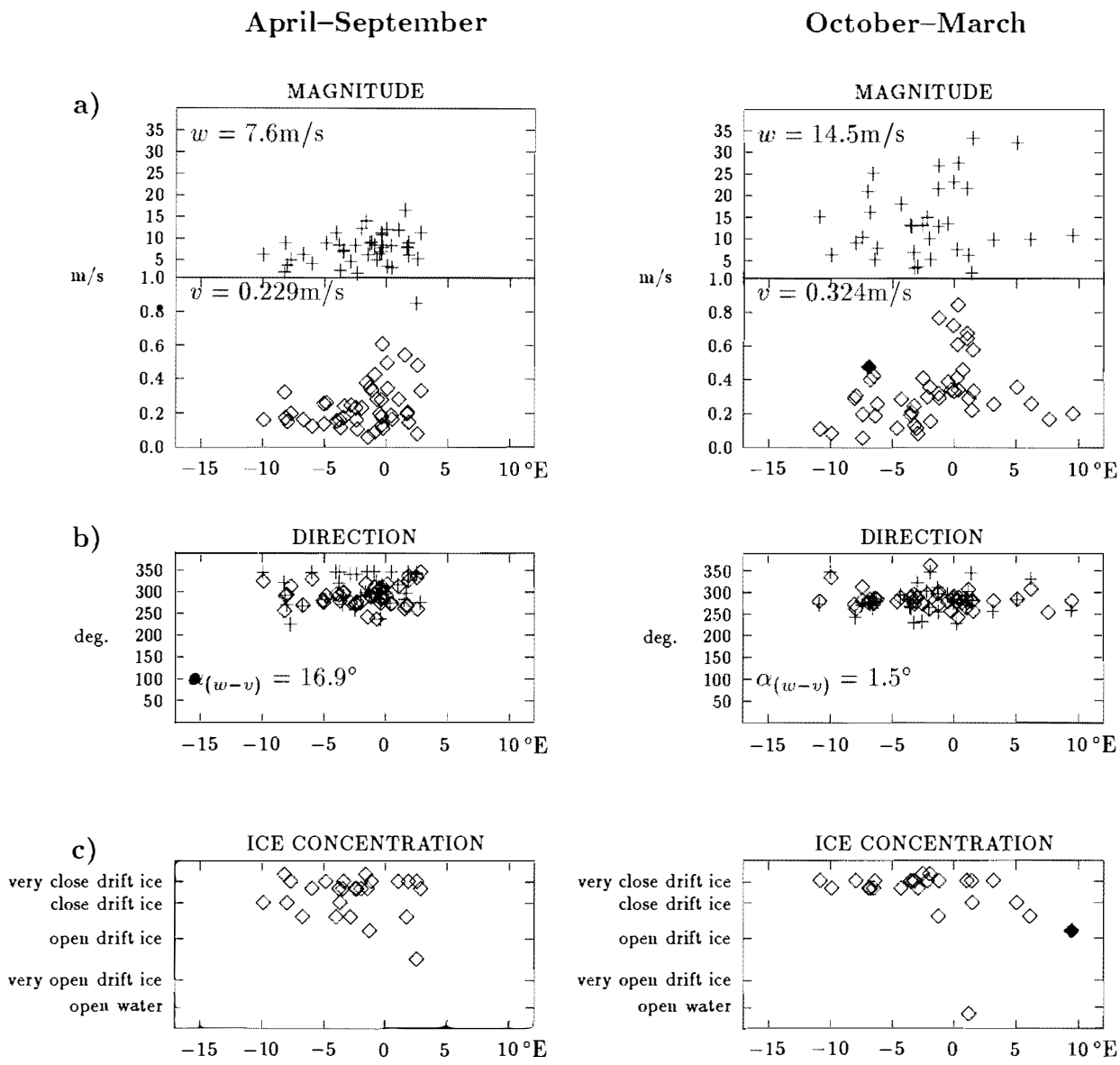

Figure 4.4: a) The magnitude and b) the direction with the stereographic x-axis of the buoy drift velocity, v (◆) and the geostrophic wind, w (+) for each buoy passing 80°N during April–September and October–March. c) The ice concentration in the neighborhood of each buoy. (Note the different annotation intervals; less than 1 (0.2m/s) and greater than 1 (5m/s)

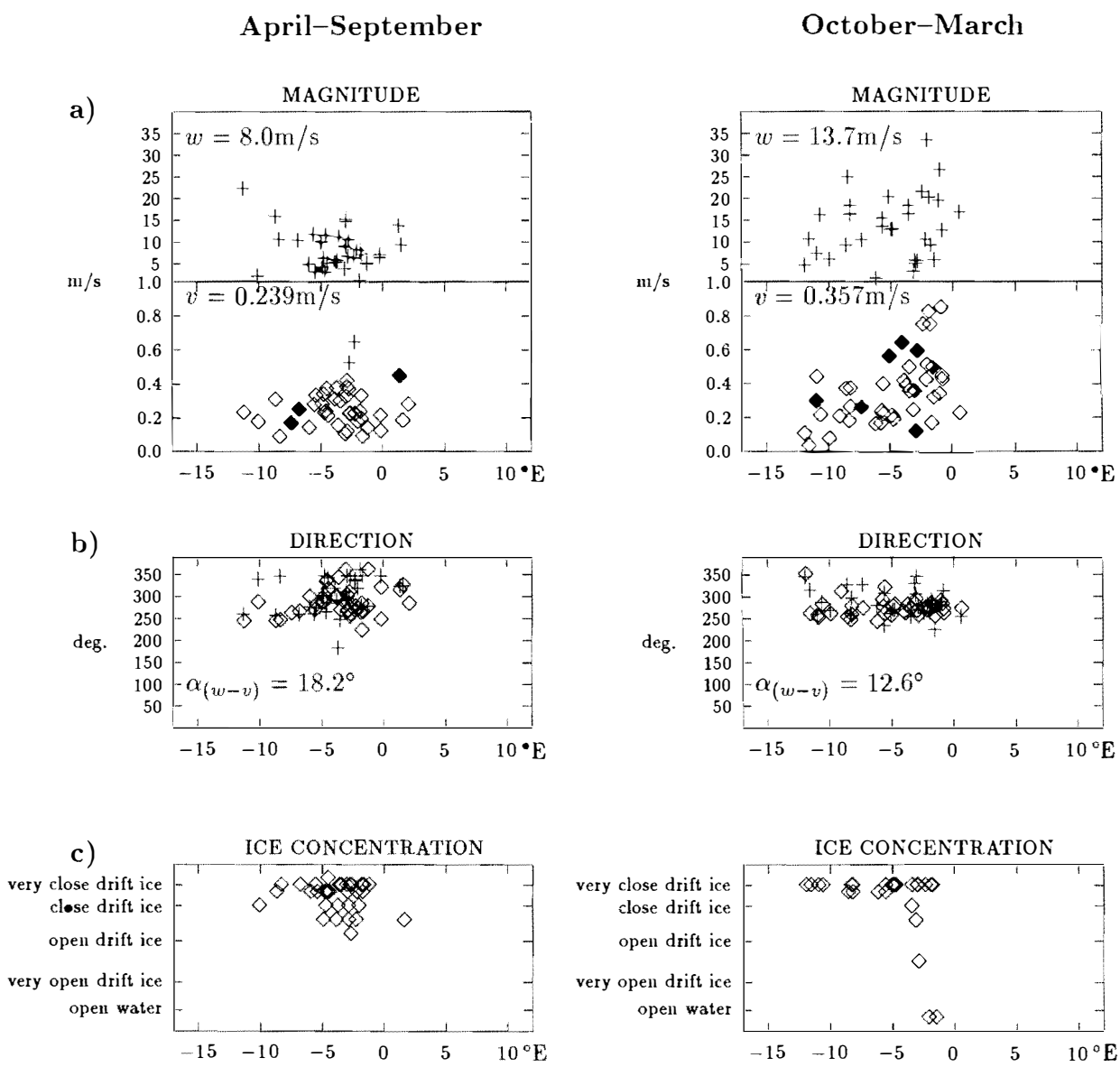

Figure 4.5: As figure 4.4, but for buoys passing 79°N.

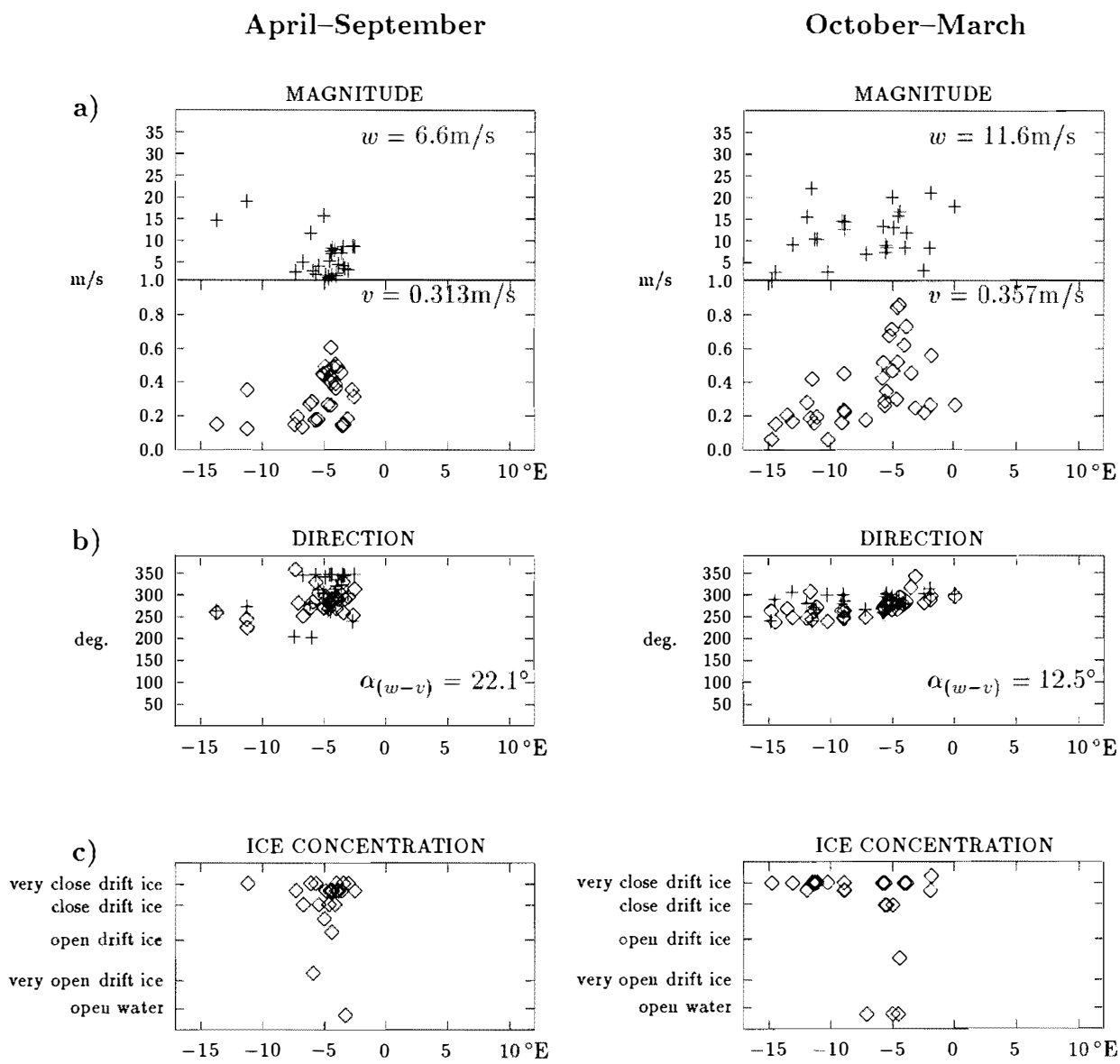

Figure 4.6: As figure 4.4, but for buoys passing 78°N.

Chapter 5

Concluding Remarks

Using data from the International Arctic Buoy Program and Norsk Polarinstitutt and the Navy–NOAA Joint Ice Center Digitalized Sea Ice Data, the drift of sea ice through the Fram Strait between Greenland and Svalbard is investigated with regard to ice drift velocity and ice distribution.
The main results are On average over the years from 1972 to 1990, the period with increasing area of ice cover in the Fram Strait starts in October and reaches a relatively stable maximum value of ice covered area in the period from December to March/April. Then the ice covered area decreases to a minimum in September. The inter annual variation can be large. During the winter season, October–March, the ice motion is fast and straight forward and can be related to the increased wind. The relatively wide ice stream have two extreme velocities equal to 0.20ms^{-1} and 0.30ms^{-1} Southward located, respectively, in between 7.5–10°W and 2.5–0°W along the 79°N-latitude (Figure 4.2). During the summer season, April–September, the ice drift is slower in a narrower and eddy structured pattern with one extreme velocity value equal to 0.18ms^{-1} Southward located in between 5–2.5°W along the 79°N-latitude (Figure 4.2). These velocity values are averaged both in time and space.

In general, the sea ice drift out of the Arctic Ocean through the Fram Strait along the East Greenland continental slope, has large interannual and seasonal variations. In view of the large seasonal variations in the ice drift velocity, ice distribution/extent, geostrophic wind, etc., one may consider quarterly or monthly mean values in future ice flux calculations.

Acknowledgments

This work was supported by the Mast-II initiative Project PL 20042, European Subpolar Ocean Program (ESOP). The authors thank The Norwegian Meteorological Institute for application of the hind cast wind database, and are grateful to T. Vinje for discussions and advice.

References

Aagard, K. & E. C. Carmack 1989: The role of sea ice and other fresh water in Arctic circulation, *J. Geophys. Res. 94,* 14485-14498.

Aleksandrov, V. Y. & R. Korsnes 1993: Ice drift in the Greenland Sea estimated from ERS-1 SAR and NOAA AVHRR images,Norsk Polarinstitutt, *Report 83,* 1-14.

Barry, R. G., M. C. Seereze, J. A. Maslanik & R. H. Preller 1993: The Arctic sea ice-climate system: observations and modeling, *Reviews of Geophysics 31* 397-422.

Breitenberger, E. 1996: The Navy/NOAA Joint Ice Center Arctic Sea Ice Data Set: An assessment of its quality and usefulness for climate research, *Journal of Climate, In Press.*

Colony, R. 1994: In WCRP-85, Initial implementation plan for the Arctic climate system study (ACSYS), WMO/TD-No.627, World Meteorological Organization, Case Postal 2300, Geneva, Switzerland.

Colony, R. & A. S. Thorndike 1985: Sea ice motion as a drunkard's walk. *J. Geophys. Res. 90,* 965-974.

Colony, R. & A. S. Thorndike 1984: An estimate of the mean field of Arctic ice motion. *J. Geophys. Res. 89,* 10623-10629.

Englebretson, R. E. & J. E. Walsh 1989: Fram Strait ice flux calculations and associated Arctic conditions. *Geojournal 18,* 61-67.

Emery, W. J., C. W. Fowler, J. Hawkins & R.H. Preller 1991: Fram Strait satellite image-derived ice motions. *J. Geophys. Res. 96* 4751-4768.

Gow, A. J. & W. B. Tucker 1987: Physical properties of sea ice discharge from Fram Strait. *Science 236* 436-439.

Hibler III, W. D. 1980: Modelling a variable thickness sea ice cover. *Mon. Weather Rev. 108* 1943-1973.

Knigth, R. W. 1984: Introduction to a New Sea Ice Database. *Annals of Glaciology 5,* 81-84.

Korsnes, R. 1994: An ice drift series from the Fram Strait January–March 1992 based on ERS-1 SAR data. *Polar Res. 13,* 55-58.

Martin, T. & P. Lemke 1995: Sea ice drift and thickness in the East Greenland Current, *Extended Abstracts*, Nordic Sea Symposium 7–9 March, Hamburg, Germany, 135-138.

Moritz, R 1988: The ice budget of the Greenland Sea. *Report APL-UWTR 8812,* Applied Physics Laboratory, University of Washington, Seattle, Washington 98105, USA.

National Snow and Ice Data Center 1996: Arctic and Antarctica Sea Ice Data, 1972-1994, on CD-ROM. Available by contacting NSIDC, URL:http://www-nsidc.colorado.edu

Sun, Y. & J. Askne 1995: An analysis of daily ice motion over Yermack Plateau. *Sensors and environmental applications of remote sensing,* (ed) J. Askne, Balkema, Rotterdam, 243-250.

Shuchman, R. A., B.A. Burns, O. M. Johannessen, E. G. Josberger, W. J. Campell, T. O. Manley & N. Lannelongue 1987: Remote sensing of the Fram Strait marginal ice zone. *Science 236,* 429-431.

Thomsen, B. B. & H. Skriver 1995: Active microwave signatures of sea ice in the Greenland Sea during summer 1993, in *Sensors and environmental applications of remote sensing,* (ed) J. Askne, Balkema, Rotterdam, 227-233.

Thorndike, A. S. & R. Colony 1982: Sea Ice motion in response to geostrophic wind. *J. Geophys. Res. 87,* 5845-5852.

Thorndike, A. S., D.A. Rothrock, G.A. Maykut & R. Colony 1975: The thickness distribution of sea ice. *J. Geophys. Res. 80,* 4501-4513.

Tucker III, W. B., A. J. Gow & W. F. Weaks 1987: Physical properties of summer sea ice in the Fram Strait. *J. Geophys. Res. 92,* 6787-6803.

Vinje, T., Nordlund, N., Østerhus, S., Korsnes, R., Kvambekk, Å & Nøst, E. 1996: Monitoring ice thickness in Fram Strait. *Approved J. Geophys Res.*

Vinje, T. 1977: Sea ice studies in the Spitsbergen-Greenland area. *Landsat Rep., E77-10206,* US Dep. of Com. Natl. Tech. Service, 5285 Port Royal, Springfield, VA.

Vinje, T. & ●. Finnekåsa 1986: The ice transport through the Fram Strait. *Norsk Polarinstitutts Skrifter 186,* 1-39.

Wadhams, P. 1992: Sea ice thickness distribution in the Greenland Sea Eurasian Basin. *J. Geophys. Res. 97,* 5331-5348.

Wadhams, P. 1983: Sea ice thickness distribution in the Fram Strait. *Nature 305,* 108-111.

Wadhams, P. 1981: The ice cover in the Greenland and Norwegian Seas. *Rev. Geophys. 19,* 345-393.

World Meteorological Organization - Commission on Marine Meteorology, 1989: Format for the Archival and Exchange of Sea Ice Data in digital Form (SIGRID), *Final Report of the 10th Session, February 1989, Recommendation 11.*

Untersteiner, N. 1988: On the ice and heat balance in the Fram Strait. *J. Geophys. Res. 93,* 527-531.